



SUPPRESSION OF SPIN WAVE INSTABILITIES
IN FERRIMAGNETS

by

CURTIS PAUL HARTWIG

S. B. , Massachusetts Institute of Technology
(1962)

S. M. , Massachusetts Institute of Technology
(1962)

SUBMITTED IN PARTIAL FULFILLMENT OF THE
REQUIREMENTS FOR THE DEGREE OF
DOCTOR OF PHILOSOPHY

at the

MASSACHUSETTS INSTITUTE OF TECHNOLOGY
May, 1966

Signature of Author

Signature redacted

Department of Electrical Engineering, May 24, 1966

Certified by

Signature redacted

Thesis Supervisor

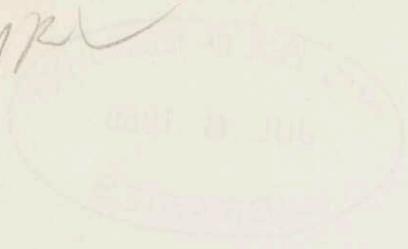
Accepted by

Signature redacted

Chairman, Departmental Committee on Graduate Students

Thesis Supervisor: Frederick R. Morgenthaler
Associate Professor of Electrical Engineering

MP



REPRODUCTION OF THE WORKS OF THE
INSTITUTE OF TECHNOLOGY

Thesis
E.E.
1966
PH.D.

MASSACHUSETTS INSTITUTE OF TECHNOLOGY
1966

SUBMITTED IN PARTIAL FULFILLMENT OF THE
REQUIREMENTS FOR THE DEGREE OF
DOCTOR OF PHILOSOPHY

BY

MASSACHUSETTS INSTITUTE OF TECHNOLOGY
1966

Signature of author
Signature of Thesis Supervisor
Signature of Departmental Committee or Graduate Schools

SUPPRESSION OF SPIN WAVE INSTABILITIES IN FERRIMAGNETS

by

CURTIS PAUL HARTWIG

Submitted to the Department of Electrical Engineering on May 24, 1966 in partial fulfillment of the requirements for the degree of Doctor of Philosophy.

ABSTRACT

This thesis presents a theoretical and experimental study of the suppression of spin wave instabilities in a ferrimagnet by the method of field modulation. Application is made to parallel pumping and "second-order" saturation of the main resonance. An experiment is described in which the cone angle of the uniform precession is opened beyond the usual instability threshold without the generation of sidebands.

Magnetic equations of motion are developed in terms of phase and amplitude for the determination of spin wave thresholds with longitudinal modulation. Suppression curves accounting for sideband generation within the spin wave spectrum are derived and fitted with a useful mathematical approximation. In the parallel pump experiment the power level for instability has been raised in excess of 10 db whereas in the excitation of the uniform precession only half this suppression is possible for the same modulation index. A mathematical model has been developed to explain deterioration of the suppression at low modulating frequencies.

Consideration is given to the application of field modulation in a parametric amplifier and a harmonic generator. A microwave power limiter with an electronically variable threshold is proposed. A preliminary investigation is made of resonant operation of the uniform precession in a disc below the spin wave manifold. It is recommended that magnetodynamic coupling between a disc and a resonator of high dielectric constant be exploited to achieve large amplitude resonance.

Thesis Supervisor: Frederic R. Morgenthaler
Title: Associate Professor of Electrical Engineering

ACKNOWLEDGEMENT

As a token of appreciation it is a pleasure to acknowledge the tutelage, advice and assistance which added to this research project.

The author wishes to thank Prof. F. R. Morgenthaler for suggesting the topic of this investigation and for many interesting and helpful discussions. Thanks are also due Profs. D. J. Epstein and H. A. Haus for their part as readers.

Over a number of years several people have made this work possible. Dr. W. Von Aulock and members of his group at Bell Telephone Laboratories introduced the author to the variety of interesting problems associated with ferrites. Association with Prof. R. L. Kyhl of M.I.T. has produced an appreciation for the relationship between microwave theory and practice. Drs. J. J. Green, R. I. Joseph, T. Kohane, and E. Schlömann of the Raytheon Research Division provided an excellent educational experience during a recent summer assignment.

Many informative discussions and comments were contributed by Messrs. J. L. Allen, H. -L. Hu, W. J. Ince, A. Platzker, S. Rezende, L. R. Tocci, M. Wanas, R. A. Williams, and Dr. W. Courtney of the Microwave and Quantum Magnetics Group. In particular, a debt of gratitude is due Dr. P. H. Cole whose advice, discussions and material aid were invaluable.

Thanks are due Miss Barbara Johnson for typing this manuscript.

Last, but by no means least, I must acknowledge my wife, Nancy, without whose patience and encouragement this work would not have been possible.

TABLE OF CONTENTS

	<u>Page</u>
ABSTRACT	3
ACKNOWLEDGEMENTS	5
TABLE OF CONTENTS	7
LIST OF SYMBOLS	9
I. Introduction	13
I. 1. High Power Instabilities	13
I. 2. Problems with Ferromagnetic Parametric Amplifiers	15
I. 3. Review of Methods of Spin Wave Suppression	17
I. 4. Organization	17
II. Spin wave Interactions and the Equations of Motion	21
II. 1. Parallel-pumping with Modulation	22
A. Derivation of the first order equations of motion	22
B. The Mechanics of Parallel Pumping	28
II. 2. Saturation of the Main Resonance	33
A. The equations of motion in an Axially Symmetric Body($\psi = 0$)	34
B. Excitation of the Second Order Instability	35
III. Suppression of the Parallel Pump Instability by Field Modulation	45
III. 1. Parallel pumping with Sinusoidal Modulation	48
A. Derivation of the Suppression Curve.	48
B. Experimental Results	52
C. Low Frequency Modulation	54
Appendix III. A. The TE_{021}^0 Cavity	57
Appendix III. B The Coil and Modulation Circuit	59
Appendix III. C The Microwave Circuit	60

	<u>Page</u>
Appendix III.D Useful Relations from Perturbation Theory	62
IV. Stabilization of the Main Resonance	77
IV. 1. A Physical Picture	77
IV. 2. Dual Modulation of the Uniform Precession in an Axially Symmetric Spheroid	78
A. Theory of the stabilized resonance	78
B. Modulation of the transverse drive	81
C. Experimental Dual Modulation	83
Appendix IV.A The TM_{120}^0 Cavity	87
Appendix IV.B The Modulation Circuit	89
Appendix IV.C Alignment Procedure	90
V. Review and Applications	99
V. 1. Evaluation of Modulation Techniques	99
V. 2. Applications of Modulation Suppression	100
V. 3. Operation below the Spin Wave Manifold	101
BIBLIOGRAPHY	103
BIOGRAPHICAL NOTE	107

LIST OF SYMBOLS

$A = A(t)$ = spin wave amplitude

$D = \lambda\omega_M$ = exchange constant

$$E = \sqrt{K_1^2 + K_2^2}$$

f = Frequency

h_{crit} = threshold amplitude of r.f. magnetic field

h_p = amplitude of pumping field

$h_{\text{r.f.}}$ = transverse driving field

$h_Z(t)$ = longitudinal modulating field

h_Z = amplitude of sinusoidal longitudinal modulating field

\vec{H} = Total magnetic field

H_C = magnitude of bias field at corner of butterfly curve

\vec{H}_i = internal bias field

$$H_i = |\vec{H}_i|$$

H_o = external field

$$H_o = |\vec{H}_o|$$

ΔH_k = spin wave half linewidth

ΔH_o = uniform precession half linewidth

$J_p(x)$ = Bessel function of the first kind

\vec{k} = spin wave wavevector

$$k = |\vec{k}|$$

$$K_1 = \frac{1}{2\omega_p} \left[\omega_k \left(\frac{\epsilon^2 + 1}{\epsilon} \right) - \frac{\omega_p^2}{2\epsilon\omega_k} \right]$$

$$K_2 = \frac{\omega_l k}{2\epsilon\omega_k}$$

\vec{M} = Total magnetization vector

$\delta\vec{M}_k$ = spin wave

$M_0 = |\vec{M}|$

M_u = uniform precession

$\delta M_x, \delta M_y, \delta M_z$ = Cartesian components of spin wave

N_t = transverse demagnetizing factor

N_z = longitudinal demagnetizing factor

P_{ic} = power incident on cavity

Q, Q_0 = unloaded Quality factor of cavity

Q_L, Q_{LO} = loaded Quality factor of cavity

Q_x = external Q

r. f. = radio frequency

t = time

T = finite averaging time

x, y, z, = Cartesian coordinates

α = phase of transverse drive

$$\alpha_0 = \tan^{-1} \frac{K_1}{K_2}$$

β, β_0 = coupling coefficient measured at cavity resonance

β_p = pump phase

β_z = phase of longitudinal field

$$\gamma = -\frac{g|e|}{2m_e} = \text{gyromagnetic ratio}$$

Γ, Γ_0 = reflection coefficient measured at cavity resonance

$$\Delta = \varphi_k - \varphi_0$$

δ = modulation index

$$\delta_z = \frac{\omega_k (1+\epsilon^2) \omega_{hz}}{\epsilon \omega_p z}$$

$$\delta' = \frac{\omega_{hZ}}{\omega_z}$$

ϵ = ellipticity

η = filling factor

θ = cone angle of uniform precession

θ_{crit} = threshold for spin wave instability

λ = exchange constant

μ_0 = permeability of free space

$$\xi = \xi(t) = \varphi - \frac{\beta_p}{2} - \frac{\alpha_0}{2}$$

$\varphi = \varphi(t)$ = slow varying phase of spin wave

$\varphi_0 = \varphi_0(t)$ = total phase of uniform precession

$\varphi_k = \varphi_k(t)$ = total phase of spin wave

$\chi = \chi' - j\chi''$ = complex magnetic susceptibility

$$\psi = \cos^{-1}(\vec{H}_i \cdot \vec{k})$$

$\omega = 2\pi f$ = radian frequency

ω_d = spin wave deviation frequency

$$\omega_h = -\gamma\mu_0 h_{\text{rf}}$$

$$\omega_{h_i} = -\gamma\mu_0 h_i$$

$$\omega_{h_p} = -\gamma\mu_0 h_p$$

$$\omega_{h_z} = -\gamma\mu_0 h_z$$

$$\omega_{h_z}(t) = -\gamma\mu_0 h_z(t)$$

$$\omega_{h_{\text{crit}}} = \gamma\mu_0 h_{\text{crit}}$$

ω_k = spin wave resonant frequency

$$\omega_{kD} = \frac{1}{2} [\omega_k - \omega_0 + \omega_M]$$

$$\omega_{lk} = -\gamma\mu_o \Delta H_k$$

$$\omega_{lo} = -\gamma\mu_o \Delta H_o$$

$$\omega_M = -\gamma\mu_o M_o$$

$$\omega_o = \omega_{Hi} + N_t \omega_M$$

$$\omega_p = \text{pump frequency}$$

$$\Omega_1 = \Omega_1(t) = \epsilon \omega_k + \omega_{h_z}(t)$$

$$\Omega_2 = \Omega_2(t) = \frac{\omega_k}{\epsilon} + \omega_{h_z}(t)$$

CHAPTER I

INTRODUCTION

This thesis is aimed at suppression of spin wave instabilities associated with ferromagnetic resonance. Motivation for this work has come from the possible application of any method of suppression to the improvement and understanding of the noise performance of ferromagnetic parametric amplifiers. Of several possible techniques, methods employing field modulation have been studied in detail. Although not necessarily optimum, they provide the possibility of turning on and off the excitation of spin waves by varying electronically the threshold for instability. Thus, in principle, one could measure the effect of spin wave excitation on the various performance characteristics of microwave ferrite devices in general - the parametric amplifier in particular.

This chapter describes the instabilities and interactions relevant to parametric amplifiers and discusses possible means for suppressing the undesirable instabilities.

I. 1 High power instabilities

Many devices make use of uniform precession of the magnetization in ferrites²². Unfortunately, above a critical power level this precession breaks up into a turbulence in the orientation of the magnetization throughout the sample. In order to explain and predict this instability threshold a number of theories have been devised^{1, 2, 3, 4, 5} in all of which the turbulence is described as a Fourier series expansion of plane waves propagating at some angle, ψ , with respect to the internal d. c. magnetic field, H_i . Each spin wave is characterized by a resonant frequency, $\omega_{\vec{k}}$, and propagation vector, \vec{k} . In an isotropic ferrimagnet the spectrum of spin wave resonant frequencies is as shown in Figure 1.1a. On an ω - k diagram, all resonant modes lie within a manifold bounded by curves along which $\psi = 0$ and $\psi = \pi/2$. This entire band can be raised in frequency by increasing the d. c. field.

Two separate processes have been described and observed^{25, 26} by which the uniform precession breaks up. From the mathematics they derive the names -"first-" and "second-order" instabilities because the pump amplitude appears to the first or second power, respectively, in the threshold equation. In the first order instability, spin waves at half the driving frequency are excited ($\omega_K \simeq \omega/2$). This process is found to have the lowest threshold at low frequencies. However, as is evident from Figure 1.1a, the frequency $\omega/2$ can be made to drop below the spin wave spectrum if the manifold of resonant modes is raised sufficiently high. In this case the first order instability has a very high threshold and becomes less likely than the second order process.

Spin waves excited by the second order process have the same frequency as the excitation ($\omega_K \simeq \omega$). In an isotropic spheroid the spin wave with the lowest threshold, and which, therefore, exhibits instability first, propagates along the internal d. c. field ($\psi = 0$). For small amplitude excitation it is to be observed that this process can never be excited below the spin wave manifold by the uniform precession at resonance.

The threshold for instability is measured in terms of the cone angle, θ , of the uniform precession. Below threshold the cone angle is a linear function of driving field. Above a critical value, θ starts to saturate as shown in Figure 1.1c. Thus, the uniform precession serves to transfer energy from the r. f. magnetic field to the spin waves.

It is actually possible to excite spin waves directly with an electromagnetic field^{3, 27}. If the r. f. magnetic field is applied along the internal field so as not to excite the uniform precession, spin waves are excited parametrically with half the frequency of the pump ($\omega_K \simeq \omega_p / 2$), provided the pump amplitude exceeds a threshold. This form of instability is referred to as parallel pumping.

Higher order transverse and parallel pump instabilities have been shown theoretically possible^{3, 5}, but have never been observed. Therefore, they will not be discussed further.

I. 2 Problems with Ferromagnetic Parametric Amplifiers

In the various parametric amplifiers that have been proposed^{10, 28, 29, 33}, the basic interaction is that of a longitudinal field (along the internal bias field, H_1) with left and right circularly polarized, transverse magnetic modes of the sample³⁴. This is shown schematically in Figure 1. 2a. Of the three interacting components any one may be pump, signal or idler. The frequencies obey the usual law: $\omega_p = \omega_s + \omega_i$. As indicated schematically in Figures 1. 2b, c, d, e, and f, the amplifiers are given various names depending on the distribution of signal (s), idler (i), and pump (p) among the three components as well as whether a magnetostatic or electromagnetic mode is dominant in the transverse modes.

Of particular importance to this work are the pump, transverse or longitudinal, how it excites spin waves and how the spin waves affect performance. In those amplifiers where the pump is a transverse mode, the threshold for amplification is determined by the cone angle, θ , as is the threshold for spin wave instability. Unfortunately, the coupling in these amplifiers has proven so weak that saturation of the pump has been a problem³⁰. A remedy must consist of raising the spin wave threshold or increasing the coupling among wanted modes to lower the amplification threshold or both.

In the longitudinally pumped magnetostatic amplifier, there is the problem of excitation of spin waves by parallel pumping which, it turns out, always have a lower threshold than that for amplification¹⁰. A remedy would require the suppression of spin wave instabilities or their avoidance by altering the amplifying modes. The latter approach is applied in the magnetodynamic amplifier³³; however, results have so far been inconclusive.

The excitation of spin waves degrades the performance of an amplifier in a number of ways. Obviously they lead to inefficient pumping. Eventually the spin waves transfer energy to the lattice as heat, thus producing thermal noise. As well, there is the

possibility that spin waves may radiate noise into the external circuitry. One other by-product is a decrease in the effective magnetization vector, \vec{M} , which results in decreased coupling and gain.

In Chapter 5 there is explored the possibility of applying modulation techniques to suppress spin wave instabilities produced by transverse or longitudinal pumping. The possibility is intriguing in that it would allow a study of the effects of spin wave instability on the gain, bandwidth and noise figure of an amplifier.

1.3 Review of methods of spin wave suppression

In the design of microwave ferrite devices the simplest and most direct means of preventing spin wave instability would be a suitable choice of materials. In particular, by making the spin wave damping much greater than that of the uniform precession, it should be possible to raise instability thresholds indefinitely. Unfortunately, the uniform precession damping always exceeds that of $k = 0$ spin waves⁴.

A number of alternative approaches have been suggested. These include removing the degeneracy between the spin wave spectrum and the resonant modes employed by the device, increasing spin wave damping by external means, or weakening the coupling between them and their pump.

If an electromagnetic and magnetostatic mode are strongly coupled, the resonant frequency of one of the resulting "magnetodynamic" modes can be designed to fall below the spin wave manifold. This interaction has been evident for samples large compared to the electromagnetic wavelength^{33,34,36}. As a result, the usual second order instability is forbidden. No information is yet available in the literature on the frequency shift and amplitude of resonance available. Work in this area is now in progress^{39,40}.

In a thin, isotropic disc magnetized normal to its plane, the uniform precession lies near the bottom of the spin wave manifold. For large amplitude resonance, the frequency of the uniform precession can, in theory³⁷, drop out of the spin wave manifold, which

when combined with modulation can exclude second-order instability. As yet no observation of on-resonance excitation below the manifold has been reported in the literature. However, in experiments in which the uniform precession was excited below its resonant frequency, it has been observed that the damping parameter changes drastically at the bottom edge of the manifold³⁵, and that below the manifold the uniform precession is limited by phonon instability.³⁸ Both experiments indicate, at least, decreased coupling to spin waves.

Instability by the "second-order process" has been suppressed with a longitudinal r.f. magnetic field³⁵. Coupling to these spin waves, which propagate along the internal field, can be produced only by altering their ellipticity through the use of a highly anisotropic material such as $Z_{n2}Y$. The suppression field must have exactly twice the frequency of the transverse driving field, which is used to establish uniform precession, and a suitable phase for depumping. Unfortunately, the longitudinal field also depumps the uniform precession because it, too, has an elliptic precession path. In this instance, the remaining problem is one of finding a suitable material which exhibits a narrow linewidth, and magnetization and anisotropy fields which are comparable.

If a longitudinal field, of frequency much less than the spin wave frequency, is applied to any ferrite, the coupling between spin wave and pump is weakened.^{13, 14, 16, 18} The same is true if the pump frequency is modulated^{15, 17}. Thus, the threshold for instability can be raised. However, if either scheme is applied to increasing the cone angle of the uniform precession, a detrimental by-product is the generation of side-bands¹⁶. This thesis describes the first successful attempt to stabilize the main resonance.

I. 4 Organization

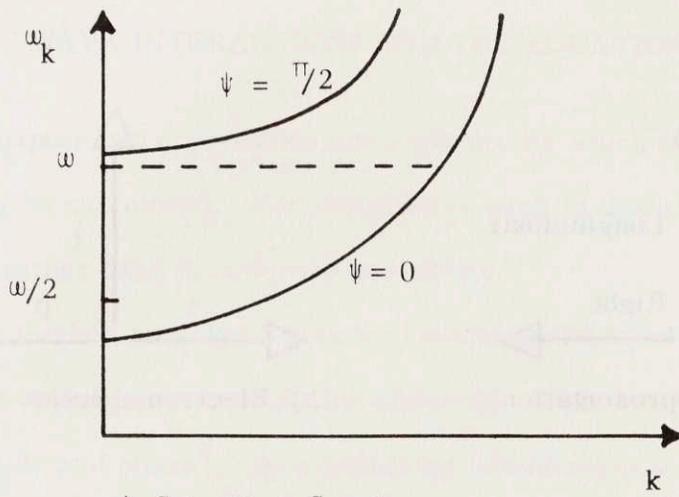
This thesis presents a theoretical and experimental study of the suppression of spin wave instabilities in a ferrimagnet by the method of field modulation. In Chapter II, the

necessary equations of motion are developed for the ensuing experiments. Thresholds for the parallel pump experiment are calculated by the method of slowly varying amplitude and phase. A description of the second order instability process is derived through the equations of motion in a rotating coordinate system. In both cases the mechanics are discussed by which spin waves are captured and driven unstable.

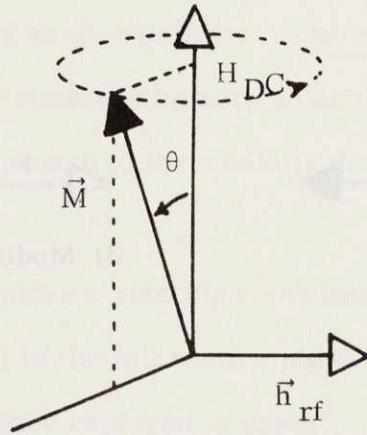
It is particularly desirable to study the mechanism by which spin waves are suppressed, without the interference of sideband generation in the uniform precession. Therefore, Chapter III has been devoted to a study of the effect of field modulation on the parallel pumping experiment. The effects of sideband generation in the spin wave spectrum are derived and verified experimentally. As is to be expected intuitively, the suppression becomes less effective as the modulation frequency is reduced below the spin wave relaxation frequency. A mathematical description is derived which suggests the correct behavior.

Operation of the uniform precession at increased cone angles and without the generation of sidebands is described in Chapter IV. A detailed study is made of the experimental apparatus and procedures necessary to achieve the desired performance.

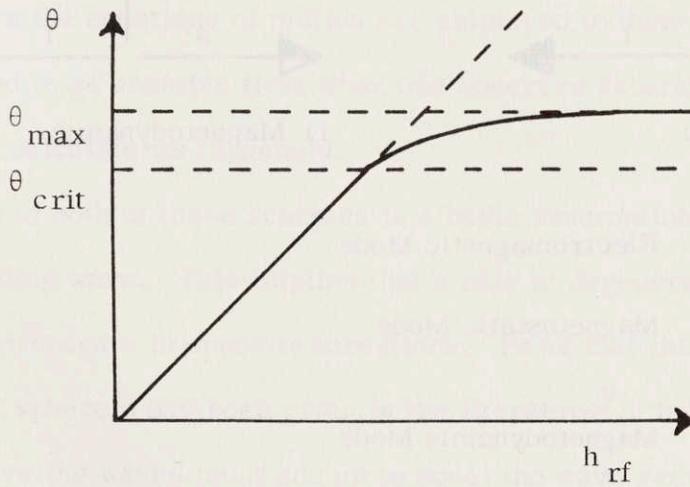
In the concluding chapter comments are made as to the possible applications of field modulation. Use of the uniform precession still creates problems because of the necessary transverse modulation. However, an interesting application appears in the form of an electronically variable parallel pump limiter. Consideration is also given to the application of field modulation in a parametric amplifier and a harmonic generator. A preliminary investigation is made of resonant operation of the uniform precession in a disc below the spin wave manifold. It is recommended that magnetodynamic coupling between a disc and a dielectric resonator of high dielectric constant be exploited to achieve large amplitude resonance.



a) Spin Wave Spectrum



b) Uniform Precession



c) Saturation of the Main Resonance

FIGURE 1.1

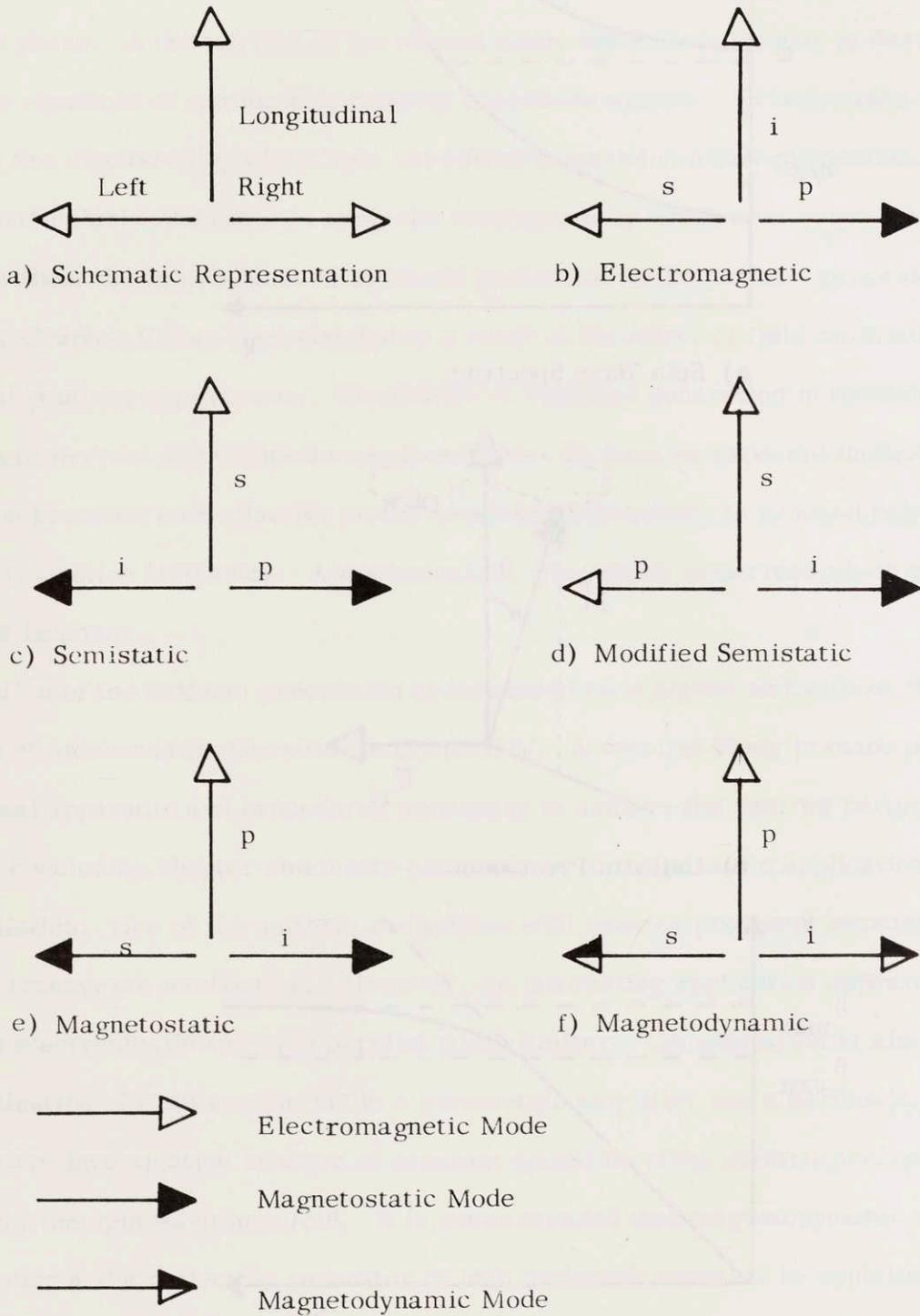


FIGURE 1.2 Ferromagnetic Parametric Amplifiers

CHAPTER II

SPIN WAVE INTERACTIONS AND THE EQUATIONS OF MOTION

In this chapter two approaches are explored by which the spin wave instability thresholds may be calculated. For simplicity, each is discussed for a specific type of experiment rather than in complete generality.

The first method employs a standard mathematical technique often used to analyze modulated waves in communication channels. This is the method of slowly-varying amplitude and phase⁶. By eliminating interactions at the microwave frequency, it becomes possible to explore, in some detail, the low frequency and transient causes and effects which lead to spin wave instability. The equations of motion are developed for the parallel pumping experiment subject to an arbitrary low-frequency longitudinal modulation. Then the approach to threshold is discussed in detail for the simple case of no modulation.

The second method employs a rotating coordinate system to make evident the modulation applied in general to the microwave phase and the amplitude of a spin wave. This method has in the past been explored in depth³. It is similar to the first method except that it includes all non-linear effects at the various microwave frequencies possible. Here the equations of motion are employed to demonstrate which spin wave can be expected to go unstable first when one observes saturation of the uniform precession and to calculate its threshold.

Common to both of these schemes is a basic assumption that the spin wave excited is a standing wave. This implies that a pair of degenerate traveling waves are caused to propagate in opposite directions. Proof that this condition is necessary in an isotropic spheroid has been given in the literature⁹. In general the wave vectors of two traveling waves must add up to equal the wave vector of the pump. If the pump is an electromagnetic wave the associated momentum is negligible compared

with that of a spin wave; whereas, if the pump is the uniform precession, the momentum is zero. Thus, for practical purposes one can write:

$$\vec{k}_1 + \vec{k}_2 = 0 \quad (2.1)$$

For \vec{k}_1 and \vec{k}_2 directed at an angle ψ_1 and ψ_2 , respectively, to the d.c. field, it is apparent that $|\vec{k}_1| = |\vec{k}_2|$ and $\sin^2 \psi_1 = \sin^2 \psi_2$. Now it is to be observed on a diagram of ω_k versus k for spin waves (see Figure 2.1) that these two restrictions define a single point within the manifold. It therefore follows that the pair of traveling spin waves must be degenerate.

Note that if one were to consider magnetostatic or magnetoelastic waves instead of spin waves, the electromagnetic momentum would not be negligible in comparison. In such cases, it is possible to excite nondegenerate pairs^{10, 11}. However, these interactions are beyond the scope of the present work.

II.1 Parallel - pumping with modulation

A. Derivation of the first-order equations of motion

The general equation of motion for a uniformly magnetized, isotropic ellipsoid is here specialized to study slow time-varying disturbances on a single spin wave excited parametrically by the "first-order process" ($\omega_k \approx \omega_p/2$).

Consider an experiment in which an isotropic ellipsoid is uniformly magnetized and both a microwave signal and a low frequency signal of arbitrary waveform are applied along the internal field (see Figure 2.2a). Orient a cartesian coordinate system such that the z-axis lies along the internal field and the x-axis coincides with the transverse component of the direction of propagation of the spin wave under consideration (see Figure 2.2b). In the magnetic equation of motion (eq. 2.5), the magnetization is assumed to consist of a static term, M_0 , and a plane wave representation of a spin wave as in eq. (2.6).

$$\dot{\vec{M}} = \gamma \mu_0 (\vec{M} \times \vec{H}) \quad (2.5)$$

$$\vec{M} = \vec{i}_z M + \delta \vec{M}_k \cos \vec{k} \cdot \vec{r} \quad (2.6)$$

The H-field consists of the internal field - H_i , the pumping field - $h_p \sin(\omega_p t + \beta_p)$, the modulation field - $h_z(t)$, and a term which varies in space - $\delta \vec{H}_k \cos \vec{k} \cdot \vec{r}$ - made up of the volume dipolar and exchange fields.

$$\vec{H} = \vec{i}_z \left[H_i + h_z(t) + h_p \sin(\omega_p t + \beta_p) \right] + \delta \vec{H}_k \cos \vec{k} \cdot \vec{r} \quad (2.7a)$$

$$\delta \vec{H}_k = \delta \vec{H} \text{ vol. dip} + \delta \vec{H} \text{ exchange} \quad (2.7b)$$

$$\nabla \cdot \delta \vec{H} \text{ vol. dip} = -\nabla \cdot \delta \vec{M}_k \quad (2.8a)$$

$$\delta \vec{H} \text{ exchange} = \lambda (\nabla^2) \vec{M} \quad (2.8b)$$

$$\delta \vec{H}_k = - \left[\vec{i}_x (\lambda k^2 + \sin^2 \psi) \delta M_x + \vec{i}_y (\lambda k^2) \delta M_y + \vec{i}_z (1/2 \sin 2\psi) \delta M_x \right] \quad (2.9)$$

Assuming a Lorentzian lineshape for the spin wave response (this is a reasonable approximation for the Landau-Lifschitz form of damping). The equations of motion are written separately for the x-and y- components of the spin wave.

$$\delta \dot{M}_x + \omega_{lk} \delta M_x = -\delta M_y \left[\Omega_1(t) + \omega_{h_p} \sin(\omega_p t + \beta_p) \right] \quad (2.10)$$

$$\delta \dot{M}_y + \omega_{lk} \delta M_y = \delta M_x \left[\Omega_2(t) + \omega_{h_p} \sin(\omega_p t + \beta_p) \right] \quad (2.11)$$

$$\delta M_z = 0 \quad (2.12)$$

The quantities Ω , and Ω_2 are slowly-varying (compared to ω_p) functions of time.

$$\Omega_1 = \omega_i + \omega_{h_z} + D k^2 = e \omega_k + \omega_{h_z} \quad (2.13)$$

$$\Omega_2 = \omega_i + \omega_{h_z} + Dk^2 + \omega_m \sin^2 \psi = \frac{\omega_k}{e} + \omega_{h_z} \quad (2.14)$$

where $\omega_i = -\gamma \mu_0 h_i$

$$\omega_{h_z} = -\gamma \mu_0 h_z(t)$$

D = convenient form of exchange constant

The first step in solving these equations is to eliminate δM_y by substituting eq. (2.10) in eq. (2.11). For convenience, replace $\omega_{h_p} \sin(\omega_p t + \beta_p)$ by $\omega_{h_p}(t)$. The complete description of motion can now be obtained from eq. (2.15).

$$\begin{aligned} \delta \ddot{M}_x + \delta \dot{M}_x \left[2\omega_{\ell k} - \frac{d}{dt} \ln(\Omega_1 + \omega_{h_p}(t)) \right] + \delta M_x \left[\omega_{\ell k} \right. \\ \left. \left\{ \omega_{\ell k} - \frac{d}{dt} \ln[\Omega_1 + \omega_{h_p}(t)] \right\} + [\Omega_1 + \omega_{h_p}(t)] [\Omega_2 + \omega_{h_p}(t)] \right] = 0 \end{aligned} \quad (2.15)$$

The approach taken here in solving this differential equation is to first note behavior with the modulation and pump turned off. Thus eq. (2.15) reduces to:

$$\delta \ddot{M}_x + 2\omega_{\ell k} \delta \dot{M}_x + (\omega_{\ell k}^2 + \omega_k^2) \delta M_x = 0 \quad (2.16)$$

This leads to the obvious pair of results for δM_x and δM_y :

$$\delta M_x = \epsilon \delta M e^{-\omega_{\ell k} t} \cos(\omega_k t + \varphi) \quad (2.17)$$

$$\delta M_y = \delta M e^{-\omega_{\ell k} t} \sin(\omega_k t + \varphi) \quad (2.18)$$

where

$$\begin{aligned} \omega_k^2 &= (\omega_i + Dk^2 + \omega_m \sin^2 \psi) (\omega_i + Dk^2) \\ \epsilon^2 &= \frac{\omega_i + Dk^2}{\omega_i + Dk^2 + \omega_m \sin^2 \psi} \end{aligned}$$

This is the usual normal mode description of spin waves as shown in Fig. 2.3.

Now expecting a solution of the form in eq. (2.17), it is reasonable to assume a solution of the form⁶:

$$\delta M_x = A(t) \cos [\omega t + \varphi(t)] \quad (2.19)$$

where $A(t)$ and $\varphi(t)$ are slowly varying functions of time, compared to the microwave signal. Considering only small perturbations on the normal modes for δM_x , one can set:

$$\dot{\delta M}_x = -A \omega \sin [\omega t + \varphi] \quad (2.20)$$

and therefore:

$$\dot{A} \cos (\omega t + \varphi) = A \dot{\varphi} \sin (\omega t + \varphi) \quad (2.21)$$

Finally:

$$\delta \ddot{M}_x = -\dot{A} \omega \sin (\omega t + \varphi) - A \omega \dot{\varphi} \cos (\omega t + \varphi) - \omega^2 \delta M_x \quad (2.22)$$

Next, multiply equation (2.15) by $\sin (\omega t + \varphi)$ and substitute in the same equations (2.19), (2.20), (2.21), and (2.22). The result is a differential equation in \dot{A} .

$$\begin{aligned} \dot{A} \omega = & - \frac{A \omega}{2} \{1 - \cos 2 (\omega t + \varphi)\} \left\{ 2 \omega_{\ell k} - \frac{d}{dt} \ln [\Omega_1 + \omega_{h_p}(t)] \right\} \\ & - \frac{A}{2} \sin 2 (\omega t + \varphi) \left\{ \omega_{\ell k} \left[\omega_{\ell k} - \frac{d}{dt} \ln [\Omega_1 + \omega_{h_p}(t)] \right] \right. \\ & \left. + [\Omega_1 + \omega_{h_p}(t)] [\Omega_2 + \omega_{h_p}(t)] - \omega^2 \right\} \end{aligned} \quad (2.23)$$

Similarly, multiply equation (2.15) by $\cos (\omega t + \varphi)$ and again substitute in the same equations, (2.19), (2.20), (2.21), and (2.22). The result is a differential equation in $\dot{\varphi}$:

$$\begin{aligned}
 A \dot{\omega} \dot{\phi} = & - \frac{A\omega}{2} \sin 2 (\omega t + \phi) \left\{ 2\omega_{\ell k} - \frac{d}{dt} \ln \left[\Omega_1 + \omega_{h_p}(t) \right] \right\} \\
 & - \frac{A}{2} \left[1 + \cos 2 (\omega t + \phi) \right] \left\{ \omega_{\ell k} \left[\omega_{\ell k} - \frac{d}{dt} \ln \{ \Omega_1 + \omega_{h_p}(t) \} \right] \right. \\
 & \left. + \{ \Omega_1 + \omega_{h_p}(t) \} \{ \Omega_2 + \omega_{h_p}(t) \} - \omega^2 \right\}
 \end{aligned} \tag{2.24}$$

It remains to eliminate the microwave frequency variation. Based on the assumption of slow variation of amplitude and phase, one can get \dot{A} and $\dot{\phi}$ by averaging one period in ω (i.e. $\frac{2\pi}{\omega}$).

$$\dot{A} \omega = \frac{\omega}{2\pi} \int_0^{\frac{2\pi}{\omega}} \left[\text{right hand side of equation 2.23} \right] dt \tag{2.25}$$

$$A \dot{\omega} \dot{\phi} = \frac{\omega}{2\pi} \int_0^{\frac{2\pi}{\omega}} \left[\text{right hand side of equation 2.24} \right] dt \tag{2.26}$$

In carrying out this averaging process, two assumptions have been made.

1. In the experiments of interest $\boxed{\omega_{h_p} \ll \Omega_1}$. This leads to two approximations:

$$\begin{aligned}
 \frac{d}{dt} \ln \left[\Omega_1 + \omega_{h_p}(t) \right] & \approx \frac{\omega_{h_p} \omega_p}{\Omega_1} \cos (\omega_p t + \beta_p) \\
 & - \frac{\dot{\Omega}_1 \omega_{h_p}}{\Omega^2} \sin (\omega_p t + \beta_p) + \frac{\dot{\Omega}_1}{\Omega_1}
 \end{aligned} \tag{2.27}$$

$$\left[\Omega_1 + \omega_{h_p}(t) \right] \left[\Omega_2 + \omega_{h_p}(t) \right] \approx \Omega_1 \Omega_2 + (\Omega_1 + \Omega_2) \omega_{h_p} \sin(\omega_p t + \beta_p) \quad (2.28)$$

2. Assume that $2\omega = \omega_p$.

Note 1: If 2ω deviates slightly from ω_p , this deviation can be taken up in φ .

Note 2: If higher order terms in $\cos n(\omega_p t + \beta_p)$ had been included one could look at $2\omega = n\omega_p$ where $n = 1, 2, 3, 4, \dots$.

The equations that result from the above averaging process are given in equations (2.29) and (2.30). Their solution is discussed in the following section and later in more depth in an investigation of suppression of spin wave instabilities by modulation.

$$\dot{\varphi} = \Lambda_1 - \frac{\omega_{h_p}}{2\omega_p} \left[\Lambda_2 \sin(2\varphi - \beta_p) + \Lambda_3 \cos(2\varphi - \beta_p) \right] \quad (2.29)$$

$$\frac{\dot{A}}{A} = \frac{\omega_{h_p}}{2\omega_p} \left\{ \Lambda_2 \cos(2\varphi - \beta_p) - \Lambda_3 \sin(2\varphi - \beta_p) \right\} - \left\{ \omega_{\ell k} - \frac{\Omega_1}{2} \right\} \quad (2.30)$$

$$\text{where } \Lambda_1 = \frac{1}{\omega_p} \left[\Omega_1 \Omega_2 + \omega_{\ell k}^2 - \frac{\omega_p^2}{4} - \frac{\omega_{\ell k} \dot{\Omega}_1}{\Omega_1} \right]$$

$$\Lambda_2 = \Omega_1 + \Omega_2 + \frac{\omega_{\ell k} \dot{\Omega}_1}{\Omega_1^2} - \frac{\omega_p^2}{2\Omega_1}$$

$$\Lambda_3 = \frac{\omega_{\ell k} \omega_p}{\Omega_1} + \frac{\omega_p \dot{\Omega}_1}{2\Omega_1^2}$$

B. The Mechanics of Parallel Pumping

As a simple application of the equations just derived, consideration is given here to the case where no modulation is applied. The mathematical behavior of spin waves at threshold is studied in some detail so that the more complicated problem with modulation can be discussed later.

With $\omega_{h_z} = 0$, the motion of a spin wave is described by equations (2.31) and (2.32).

$$\dot{\varphi} = \omega_d - \omega_{h_p} \left[K_1 \sin(2\varphi - \beta_p) + K_2 \cos(2\varphi - \beta_p) \right] \quad (2.31)$$

$$\frac{\dot{A}}{A} = \omega_{h_p} \left[K_1 \cos(2\varphi - \beta_p) - K_2 \sin(2\varphi - \beta_p) \right] - \omega_{\ell k} \quad (2.31)$$

where
$$\omega_d = \frac{1}{\omega_p} \left[\omega_k^2 + \omega_{\ell k}^2 - \frac{\omega_p^2}{4} \right]$$

$$K_1 = \frac{1}{2\omega_p} \left[\omega_k \left(\frac{\epsilon^2 + 1}{\epsilon} \right) - \frac{\omega_p^2}{2\epsilon\omega_k} \right]$$

$$K_2 = \left[\frac{\omega_{\ell k}}{2\epsilon\omega_k} \right]$$

It is convenient at this point to introduce a change in the definition of the phase of interest in order to simplify the equations of motion.

$$2 \xi(t) = 2 \varphi(t) - \beta_p - \alpha_0 \quad (2.23)$$

where $\tan \alpha_0 = \frac{K_1}{K_2}$

The equations of interest can now be written:

$$\dot{\xi} = \omega_d - \omega_{hp} E \cos 2\xi \tag{2.34}$$

$$\frac{\dot{A}}{A} = -\omega_{hp} E \sin 2\xi - \omega_{lk} \tag{2.35}$$

where $E = \sqrt{K_1^2 + K_2^2}$

Before attempting a solution of these equations consider their physical interpretation. If one considers a spin wave whose natural frequency deviates slightly from $\omega_{p/2}$ such that:

$$\sqrt{\omega_k^2 + \omega_{lk}^2} = \frac{\omega_p}{2} + \delta$$

where $\delta \ll \frac{\omega_p}{2}$

then $\omega_k^2 + \omega_{lk}^2 \approx \frac{\omega_p^2}{4} + \omega_p \delta$

or $\frac{1}{\omega_p} \left[\omega_k^2 + \omega_{lk}^2 - \frac{\omega_p^2}{4} \right] = \delta = \omega_d$

That is, ω_d , in fact, the deviation of $\omega_{p/2}$ from the natural frequency of any spin wave. Thus, consideration is given to any individual spin wave over a narrow range.

Because ξ is independent of A in the above equations it can be solved first and then used to study A. The equation in A can be rewritten as:

$$A = A_0 e^{-\omega_{lk} t} e^{-\omega_{hp} E \int \sin 2\xi dt} \tag{2.36}$$

Obviously A decays unless $\int \sin 2\xi dt$ has a term of the form Kt. This is true only if $K = \langle \sin 2\xi \rangle$. Therefore, the condition of stability is determined by:

$$\left\langle \frac{\dot{A}}{A} \right\rangle = -\omega_{hp} E \langle \sin 2\xi \rangle - \omega_{lk} \quad (2.37)$$

At the threshold, $\left\langle \frac{\dot{A}}{A} \right\rangle = 0$ and so:

$$\omega_{h \text{ crit.}} = - \frac{\omega_{lk}}{E \langle \sin 2\xi \rangle} \quad (2.38)$$

Now the question arises as to whether the threshold condition can be met. The following steps demonstrate the conditions for instability.

Mathematically there are two forms of solution for the equation in ξ , depending on whether ω_d^2 is greater or less than $\omega_{hp}^2 E^2$. Case A $\omega_d^2 > \omega_{hp}^2 E^2$

Direct integration of equation (2.34) gives the solution:

$$\tan \xi = \epsilon_1 \tan(\omega_q t + \alpha) \quad (2.39)$$

$$\text{where } \epsilon_1 = \sqrt{\frac{\omega_d^2 - \omega_{hp}^2 E^2}{\omega_d^2 + \omega_{hp}^2 E^2}} \quad 0 \leq \epsilon_1 \leq 1$$

$$\omega_q = \sqrt{\omega_d^2 - \omega_{hp}^2 E^2} \quad 0 \leq \omega_q \leq \omega_d$$

The quantity ξ can be written as:

$$\xi = \omega_q t + \alpha + f(t)$$

$$\text{where } \tan f = \frac{(\epsilon_1 - 1) \tan(\omega_q t + \alpha)}{1 + \epsilon_1 \tan^2(\omega_q t + \alpha)} \quad -\frac{\pi}{2} < f(t) < +\frac{\pi}{2}$$

To evaluate the growth of A, observe $\sin 2\xi$:

$$\sin 2\xi = \frac{2 \epsilon_1 \sin 2(\omega_q t + \alpha)}{(1 + \epsilon_1^2) + (1 - \epsilon_1^2) \cos 2(\omega_q t + \alpha)}$$

This is an odd function of time and, therefore, has a zero average value. Thus, it is obvious that, while initially there will be a fluctuation in the amplitude of the spin waves which satisfy $\omega_d^2 > \omega_{hp}^2 E^2$, the amplitudes decay and no instability is observed.

The conditions described in Case A imply that the spin waves are not Phase-locked. Now consider the more interesting case in which instability can occur.

Case B $\omega_d^2 < \omega_{hp}^2 E^2$

Direct integration now leads to the result:

$$\frac{\sin q \cdot \sin 2\xi}{1 - \cos q \cos 2\xi} = \tanh(2\alpha_q T) \quad (2.40)$$

where $\omega_{hp} E \cos q = \omega_d$

$$\omega_{hp} E \sin q = -\alpha_q$$

$$\alpha_q = \sqrt{\omega_{hp}^2 E^2 - \omega_d^2}$$

Here the angle 2ξ grows from 0 to $-q$ as time proceeds from initial turn on. Thus, for large t :

$$\frac{\dot{A}}{A} = \alpha_q - \omega_{lk} = \sqrt{\omega_{hp}^2 - \omega_d^2} - \omega_{lk} \quad (2.41)$$

and is constant.

Thus, a threshold for instability occurs if

$$\alpha_q = \omega_{lk} \quad \text{or} \quad \omega_{h_{crit}} = \frac{\sqrt{\omega_d^2 + \omega_{lk}^2}}{E} \quad (2.42)$$

It is conceivable that some information has been lost about a transient buildup. However,

the mathematical difficulties prevent a thorough analysis.

Now, notice what has happened. A spin wave for which

$$\sqrt{\omega_k^2 + \omega_{lk}^2} = \frac{\omega_p}{2} + \omega_d$$

has been captured (phase-locked) and after a finite time is driven at $\omega_p/2$. That is, observe that $\dot{\xi}$ changes from ω_d to zero as a function of time and stays phase-locked.

It is helpful to go a few steps in evaluating the threshold given above.

$$K_1 = \frac{1}{2\omega_p \epsilon} \left[\omega_k \epsilon^2 - \omega_k - \frac{2\omega_{lk}^2}{\omega_k} + \frac{2\omega_p \omega_d}{\omega_k} \right]$$

In the case of interest where YIG is the material considered:

$$K_1 \approx \frac{\epsilon^2 - 1}{4\epsilon} \gg K_2 = \frac{\omega_{lk}}{2\epsilon\omega_k}$$

$$\therefore E = |K_1| = \frac{1 - \epsilon^2}{4\epsilon}$$

so the threshold may be written as:

$$\omega_{h \text{ crit}} = \frac{4\epsilon \sqrt{\omega_{lk}^2 + \omega_d^2}}{1 - \epsilon^2} \quad (2.43)$$

or, equivalently

$$\omega_{h \text{ crit}} = \frac{\omega_p \sqrt{\omega_{lk}^2 + \omega_d^2}}{\omega_m \sin^2 \psi} \quad (2.44)$$

These expressions are in agreement with previous results. Note that because the only important threshold is the lowest, $\omega_{h \text{ crit}}$ can be written, practically, as:

$$\omega_{h_{crit}, \min} = \text{Min} \left\{ \frac{\omega_p (2\omega_{\ell k})}{\omega_m \sin^2 \psi} \right\} \quad (2.45)$$

To summarize it is convenient to use a diagram such as shown in Fig. 2.4a. As the pump amplitude is increased an ever larger band of spin waves are phase-locked. Experimentally this is exhibited as a loss term in the susceptibility, χ'' , which increases gradually from a finite value at $\omega_{hp} = 0$ to a very much larger value when $\omega_{hp} = \omega_{h_{crit}}$. This has been observed and reported in the literature¹². The threshold is determined by the first spin wave to go unstable. Above threshold, no information is available from the present analysis because of the multiple interactions involved.

When measured versus applied magnetic field the threshold in an isotropic sample exhibits the behavior shown in Fig. 2.4b. It is to be noted in equation (2.45) that the minimum threshold occurs for $\psi = \pi/2$ where possible. This does occur for $H_0 \leq H_c$. The behavior exhibited is directly proportional to $\omega_{\ell k}$ as a function of k on the top of the spin wave manifold of Fig. 2.3a. For $H_0 > H_c$ it is impossible for ψ to remain equal to $\pi/2$. As H_0 increases ψ decreases and the threshold curve is determined by ψ and $\omega_{\ell k}$ versus ψ for $k \rightarrow 0$.

II.2 Saturation of the Main Resonance

In the review of high power instabilities of chapter one, it was pointed out that the "first order process" in which $\omega_k = \omega/2$ is forbidden if ω is higher than a critical frequency, ω_c . In an isotropic spheroid magnetized along its axis of symmetry, this critical

frequency is given by:

$$\omega_c = 2N_t \omega_M \quad (2.50)$$

where N_t is the transverse demagnetizing factor. If the material is YIG, the highest critical frequency occurs for a rod and is approximately 5 Gc. In the experiments that follow, excitation is always above 8 Gc. Therefore, this instability is forbidden and will not be explored further.

It has been shown^{1,2,3} that the lowest threshold for the "second order process" ($\omega_k = \omega$) occurs for spin waves propagating along the d. c. magnetic field ($\psi = 0$). This is the instability expected in the experiments on saturation of the main resonance. The

purpose of this section is to present the equations of motion in a rotating coordinate system for the uniform precession and a spinwave, then to solve these equations for a description of the saturation process.

A. The equations of motion in an axially symmetric body ($\psi = 0$) ³

For small amplitude resonance, with which this thesis is concerned, the uniform precession can be described in terms of a cone angle, θ , and a phase, φ_0 , as in Fig. 2.5a and equation (2.51).

$$\vec{M} = M \theta (\vec{i}_x \cos \varphi_0 + \vec{i}_y \sin \varphi_0) \quad (2.51)$$

When excited by circularly polarized magnetic fields of amplitude, h_i , and frequency ω_i , as in Fig. 2.5b, and longitudinal fields, h_j , of frequency, ω_j , the phase and cone angle are described by a pair of differential equations.

$$\dot{\varphi}_0 = \omega_0 - \frac{1}{\theta} \sum_i \omega_{h_i} \cos (\omega_i t - \varphi_0 + \alpha_i) + \sum_j \omega_{h_{z_j}} \sin (\omega_j t + \beta_j) \quad (2.52)$$

$$\dot{\theta} = \sum_i \omega_{h_i} \sin (\omega_i t - \varphi_0 + \alpha_i) - \omega_{\ell_0} \theta \quad (2.53)$$

The resonant frequency is given by $\omega_0 = \omega_{H_i} + N_t \omega_M$, and the relaxation frequency is ω_{ℓ_0} . In this analysis emphasis is placed on the behavior of the uniform precession only up to the threshold of spin wave excitation; therefore, no spin wave reaction terms are included in the above equations.

A standing spin wave is described in terms of its amplitude, δM , and phase,

$$\vec{M}_k = \delta M (\vec{i}_x \cos \varphi_k + \vec{i}_y \sin \varphi_k) \cos \vec{k} \cdot \vec{r} + \vec{i}_z \delta M_z \quad (2.54)$$

For propagation along the d. c. field ($\psi = 0$) motion of the spin wave is also described

by two differential equation.

$$\dot{\varphi}_K = (\omega_K + \omega_{KD} \theta^2) + \omega_{KD} \theta^2 \cos 2(\varphi_K - \varphi_0) + \sum_j \omega_{h_z_j} \sin(\omega_j t + \beta_j) \quad (2.55)$$

$$\delta \dot{M} = \left\{ \theta^2 \omega_{KD} \sin 2(\varphi_K - \varphi_0) - \omega_{Lk} \right\} \delta M \quad (2.56)$$

where

$$\omega_{KD} = \frac{1}{2} \left[Dk^2 + \omega_M(1-N_t) \right] = \frac{1}{2} \left[\omega_K - \omega_0 + \omega_M \right]$$

The spin wave resonant frequency is given by $\omega_K = \omega_{H_i} + Dk^2$. Note that the spin wave is influenced by the phase and amplitude of the uniform precession and by the longitudinal fields, but not by the transverse fields.

In general, any magnetic field excitation of the sample can be described in terms of right and left circularly polarized fields and longitudinal fields. The above equations, then, constitute a complete description for the assumed model under arbitrary excitation.

In the following section, these equations are solved for the case in which the uniform precession is driven by a single circularly polarized r. f. magnetic field.

B. Excitation of the second order instability

Consider a spheroid magnetized along its axis and excited by a transverse circularly polarized field of frequency ω .

$$\vec{h} = h \left[\vec{i}_x \cos(\omega t + \alpha) + \vec{i}_y \sin(\omega t + \alpha) \right] \quad (2.57)$$

The uniform precession is described by two equations.

$$\dot{\varphi}_0 = \omega_0 - \frac{1}{\theta} \omega_h \cos(\omega t - \varphi_0 + \alpha) \quad (2.58)$$

$$\dot{\theta} = \omega_h \sin(\omega t - \varphi_0 + \alpha) - \omega_{\ell 0} \theta \quad (2.59)$$

In the steady state, the uniform precession moves with phase $\varphi_0 = \omega t$ which lags behind the transverse driving field by the angle α .

$$\cos \alpha = \frac{\omega_0 - \omega}{\sqrt{(\omega_0 - \omega)^2 + \omega_{\ell 0}^2}} \quad (2.60)$$

$$\sin \alpha = \frac{\omega_{\ell 0}}{\sqrt{(\omega_0 - \omega)^2 + \omega_{\ell 0}^2}} \quad (2.61)$$

The cone angle opens to a steady value.

$$\theta = \frac{\omega_h}{\sqrt{(\omega_0 - \omega)^2 + \omega_{\ell 0}^2}} \quad (2.62)$$

Under the conditions described here, consider the motion of a spin wave. For convenience replace $\varphi_k - \varphi_0 = \varphi_k - \omega t$ by Δ . Equations (2.55) and (2.56) become:

$$\dot{\Delta} = (\omega_K + \omega_{KD} \theta^2 - \omega) + \omega_{KD} \theta^2 \cos 2 \Delta \quad (2.63)$$

$$\delta \dot{M} = \left\{ \theta^2 \omega_{KD} \sin 2 \Delta - \omega_{\ell k} \right\} \delta M \quad (2.64)$$

The form of these equations is the same as equations (2.34) and (2.35) used to describe parallel pumping. Once again there is a region of phase lock and a region of instability. However there is a subtle difference. The time invariant term in equation (2.63) contains the pump amplitude, θ .

The region outside of phase lock has been explored in some detail in the literature⁸ and is not pursued here. It is to be noted that phase lock occurs only if:

$$\omega > \omega_K > \omega - 2\omega_{KD} \theta^2 \quad (2.65)$$

In the steady state $\dot{\Delta} = 0$ and so $\cos 2\Delta$ and $\sin 2\Delta$ are determined.

$$\cos 2\Delta = \frac{\omega - \omega_K - \omega_{KD} \theta^2}{\omega_{KD} \theta^2} \quad (2.66)$$

$$\sin 2\Delta = \frac{\sqrt{(\omega - \omega_K)(\omega_K - \omega + 2\omega_{KD} \theta^2)}}{\omega_{KD} \theta^2} \quad (2.67)$$

Instability occurs if $\delta \dot{M} \geq 0$.

$$\theta_{\text{crit}}^2 = \frac{1}{\omega_{KD}} \left\{ (\omega - \omega_K) + \frac{\omega_{\ell k}^2}{(\omega - \omega_K)} \right\} \quad (2.68)$$

This is a minimum for $\omega - \omega_K = \omega_{\ell k}$.

$$\theta_{\text{crit, min}}^2 = \frac{2\omega_{\ell k}}{\omega_{KD}} \approx \frac{2\omega_{\ell k}}{\omega_M}$$

An important feature of this solution, as shown in Fig. 2.6, is that the resonant frequency of any spin wave driven unstable must lie below the driven unstable must lie below the driving frequency.

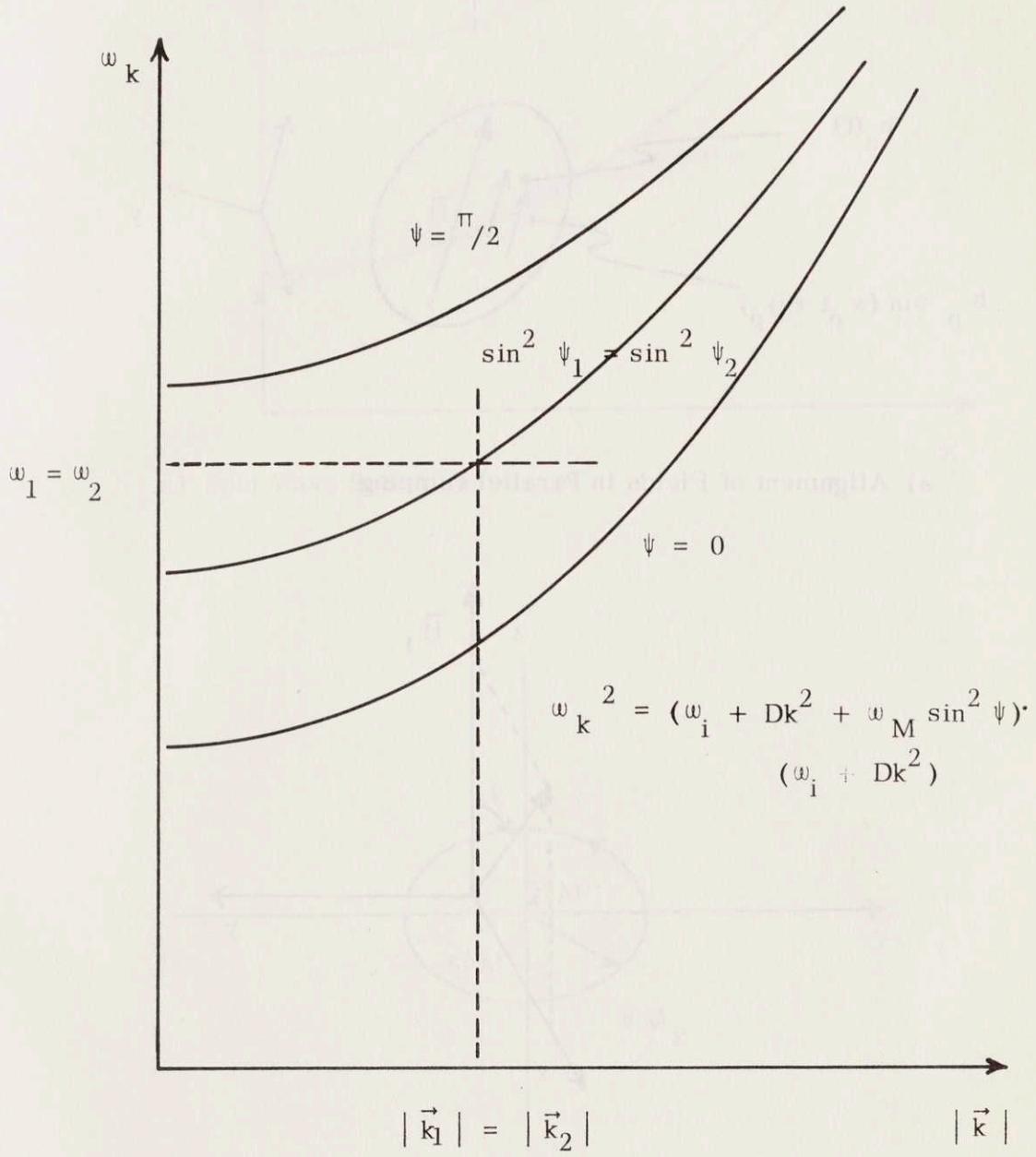
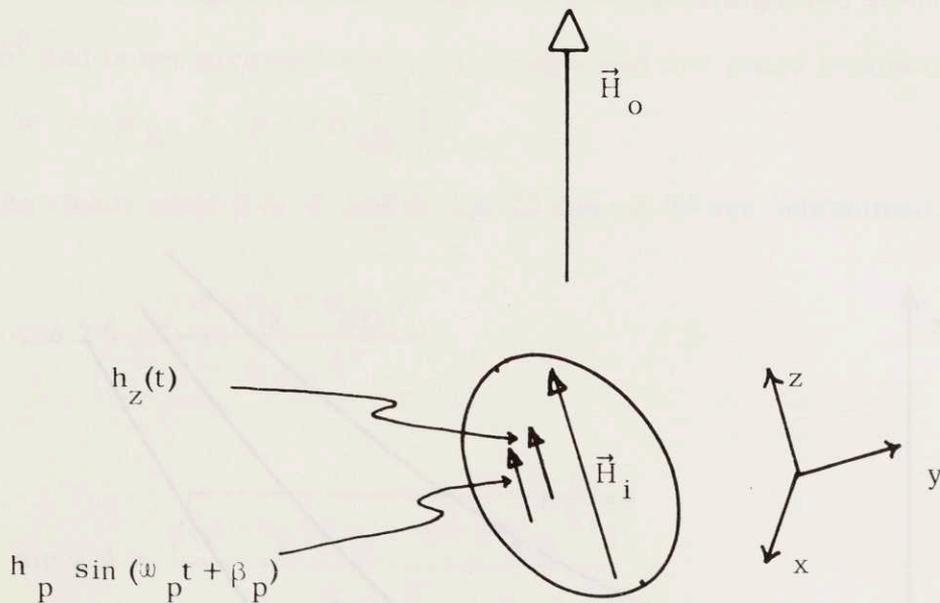
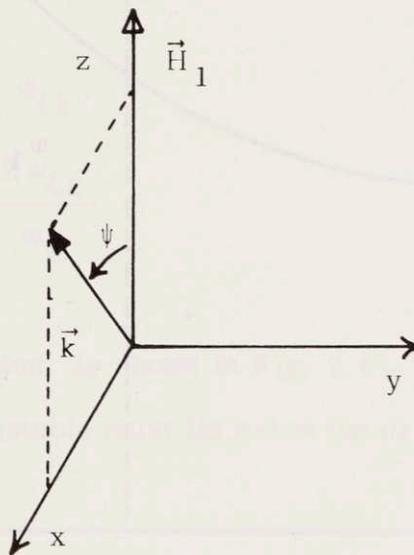


FIGURE 2.1

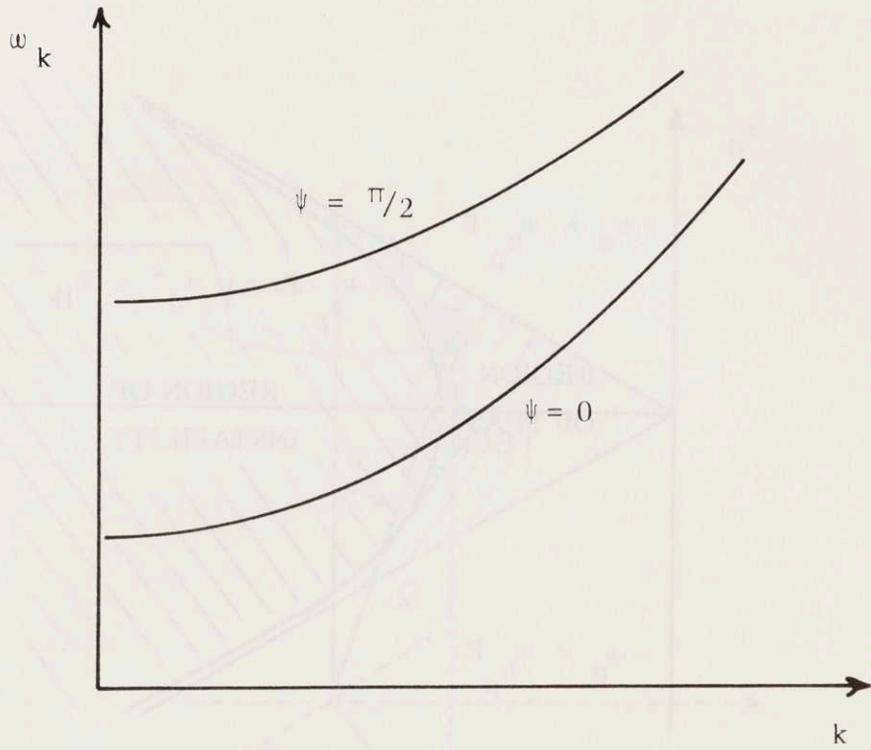


a) Alignment of Fields in Parallel Pumping

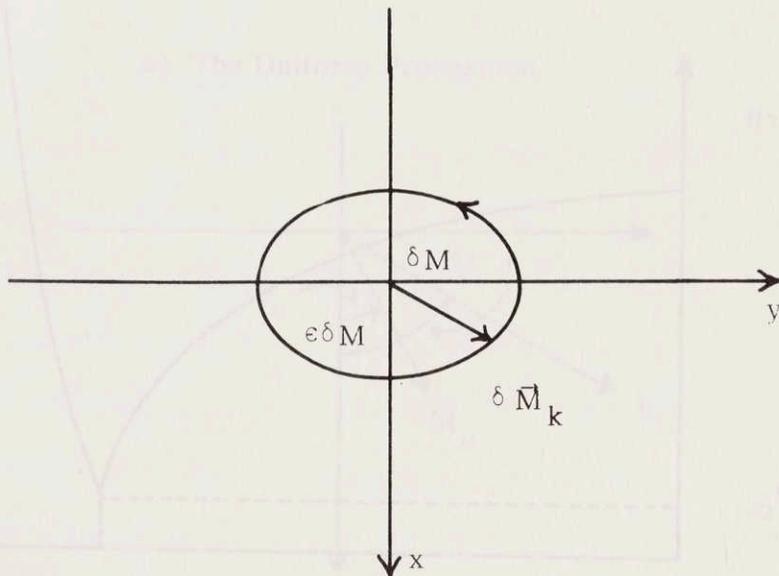


b) Orientation of wavevector, \vec{k} .

FIGURE 2.2

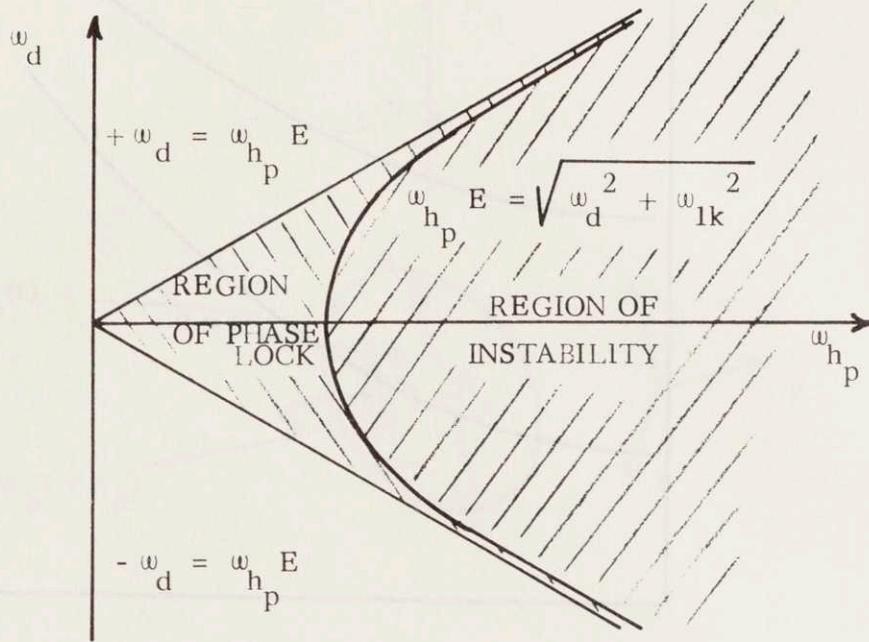


a) Spin Wave Spectrum

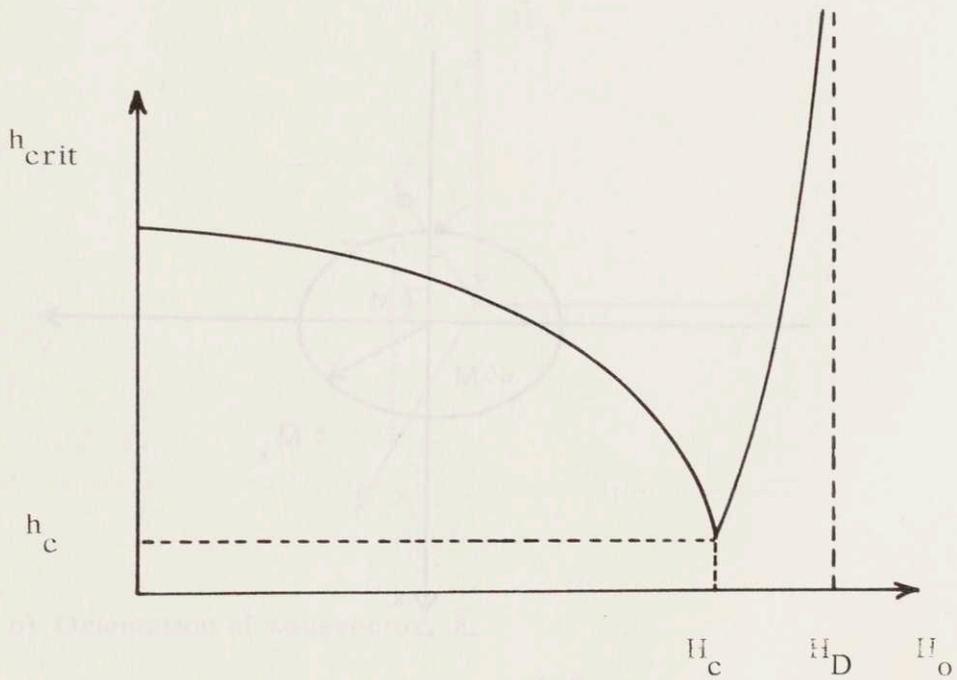


b) Precession Path

FIGURE 2.3

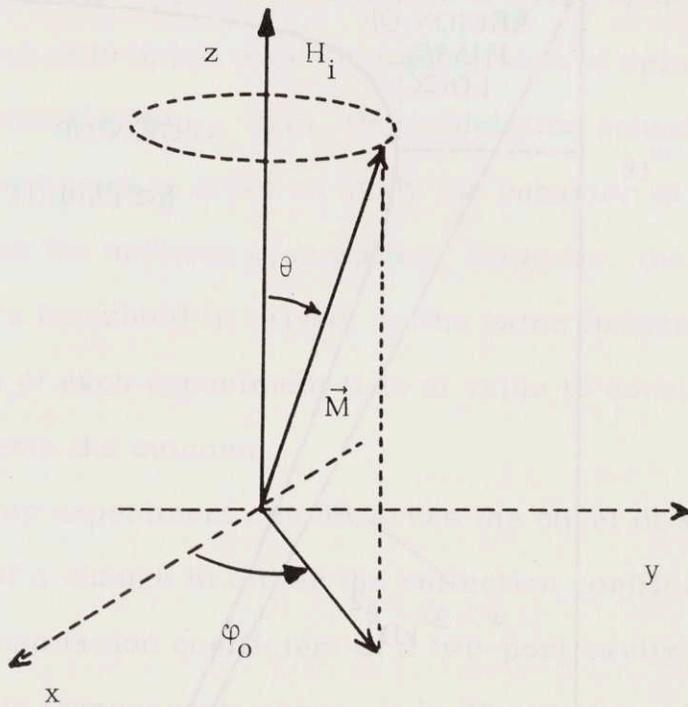


a) Stability Diagram

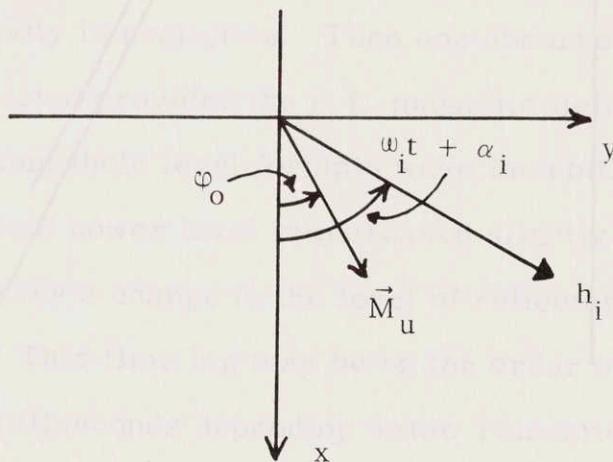


b) Butterfly Curve

FIGURE 2.4



a) The Uniform Precession



b) The Transverse Plane

FIGURE 2.5

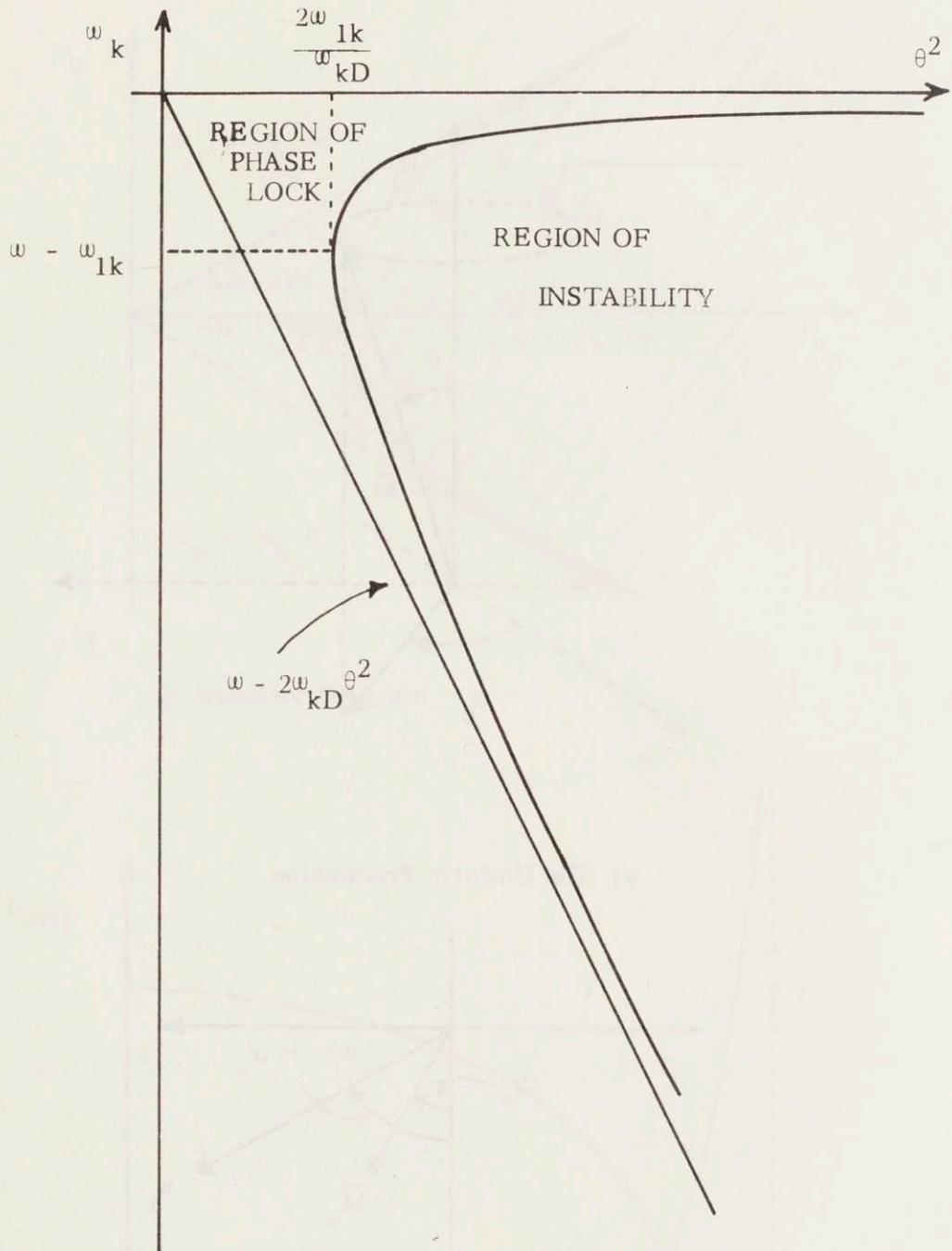


FIGURE 2.6



77 Massachusetts Avenue
Cambridge, MA 02139
<http://libraries.mit.edu/ask>

DISCLAIMER NOTICE

Due to the condition of the original material, there are unavoidable flaws in this reproduction. We have made every effort possible to provide you with the best copy available.

Thank you.

The following pages were not included in the original document submitted to the MIT Libraries.

This is the most complete copy available.

p. 44

CHAPTER III
SUPPRESSION OF THE PARALLEL PUMP INSTABILITY
BY FIELD MODULATION

In this and the following chapter, an analysis is given of theoretical and experimental problems associated with the suppression of spin wave instabilities by field modulation. Here, the modulation scheme is applied to the parallel pump experiment in order to study the behavior of spin waves free of interaction with the uniform precession. However, the basic mechanism, by which the spin wave threshold is raised, is the same in both cases. Before discussing the details of each experiment it is of value to consider an intuitive argument which suggests the outcome.

In the parallel pump experiment one observes the onset of spin wave instability by means of a change in either the reflection coefficient of a one-port cavity or the transmission coefficient of a two-port cavity. Below threshold the sample is transparent; above, it is dissipative. Consider, for example, an undercoupled one-port cavity. With reference to Figure 3-1a, assume that at $t = 0$, the incident power is turned on to a constant value and that ringing of the cavity is negligible. Then one observes that the reflected power remains unaffected provided the r. f. magnetic field applied to the sample is below the threshold level for spin wave instability (i. e. $h_1 < h_{crit}$). However, if the incident power level is increased slightly above threshold ($h_2 > h_{crit}$) one observes a change in the level of reflected power after a finite interval of time, t_0 . This time lag may be on the order of tens of microseconds to units of milliseconds depending on the relaxation rate of the initial spin wave excited.

Now suppose the frequencies of the pump and the spin wave manifold are

somehow changed relative to one another before time, t_0 . The initial spin wave cannot grow if the pump power no longer exceeds its threshold, which is determined in part by $\omega_d \cong (\omega_k - \omega_p/2)$. Excitation is transferred to another spin wave and the process can be carried on ad infinitum. The resultant observation is an increase in threshold power, resulting from weakened coupling to the spectrum of spin waves.

The process described can be carried out in practice by varying either the excitation frequency or the resonant frequencies of the spin waves. The latter scheme requires that the bias field be modulated. Thus the pumping energy is distributed over a wide band and, if the rate of change is sufficiently rapid, no spin wave should be excited long enough to go unstable.

In the initial theoretical work¹³ on this mechanism, it was believed that one could eliminate the spin wave instabilities entirely with sufficient modulation. Preliminary experiments using field modulation^{14, 18} and frequency modulation¹⁵ appeared to confirm this belief but only because the extent of modulation in each case was extremely small. It was later recognized¹⁶ that either form of modulation will produce sideband excitation. That is, consider for example a frequency modulated r. f. magnetic field used as pump.

$$h = h_0 \sin [\omega_p t + \beta_p + \delta \cos (\omega_m t + \beta_m)] \quad (3.1)$$

While, in fact, this is the form of modulation one would expect to use for suppression, it can be looked upon in an alternate form as the sum of an infinite number of magnetic fields at the sideband frequencies, $\omega_p \pm n \omega_m$ for all integer values of n . Evidently there are not just one but an infinite number of pumps, each of which can create an instability if it exceeds the

threshold. This has been confirmed in experiments employing frequency modulation of the pump.¹⁷ In a like manner, modulation of the spin wave spectrum causes each spin wave to be resonant not only at its center frequency but also at sideband frequencies, $\omega_k \pm n \frac{\omega_m}{2}$. Thus the extent to which instabilities can be suppressed must be investigated mathematically and experimentally.

III-1. Parallel Pumping with Sinusoidal Modulation

A. Derivation of the suppression curve

In this section a study is made of the extent to which the threshold for parallel pump instability can be raised when the sample is subject to a single frequency longitudinal modulation.

$$\omega_{hz}(t) = \omega_{hz} \sin(\omega_z t + \beta_z) \quad (3.3)$$

where

$$\omega_{hz} = -\gamma \mu_0 h_z$$

It is assumed that both the modulation frequency, ω_z , and the term ω_{hz} are much less than the pump and spin wave frequencies.

$$\omega_{hz} \ll \epsilon \omega_k < \frac{\omega_k}{\epsilon} < \omega_p \quad (3.4a)$$

and

$$\omega_z \ll \omega_k < \omega_p \quad (3.4b)$$

Under the conditions of equation (3.4a), the parallel pump equations of motion, equations (2.29) and (2.30) can be reduced to a form similar to equations (2.34) and (2.35).

$$\begin{aligned} \dot{\xi} &= \omega_d + \omega_z \delta_z \sin(\omega_z t + \beta_z) \\ &\quad - \omega_{hp} E \cos 2\xi \end{aligned} \quad (3.5)$$

$$\frac{\dot{A}}{A} = -\omega_{hp} E \sin 2\xi - \omega_{lk} \quad (3.6)$$

where

$$\delta_z = \frac{\omega_k (1 + \epsilon^2) \omega_{hz}}{\epsilon \omega_p \omega_z}$$

It is to be noted that the only significant effect of the modulation is that of phase modulating the spin wave.

Once again the obvious approach to a solution for an instability threshold is a) to solve equation (3.5) for ξ , b) compute the time average of $\sin 2\xi$ and c) observe the amplitude of the pump, ω_{hp} , at which there is time average growth in the amplitude of the spin wave, A. Unfortunately, because of mathematical difficulties, an exact solution of equation (3.5) is not readily found. However, from equation (2.38) note the relative amplitudes of $\omega_{hp} E$ and ω_k at the threshold.

$$|\omega_{hp} E| = \left| \frac{\omega_{lk}}{\langle \sin 2\xi \rangle} \right| \geq \omega_k \quad (3.7)$$

Now if $\omega_z \delta_z \gg |\omega_{hp} E| > \omega_{lk}$, one can write a good approximation to equation (3.5).

$$\dot{\xi} \cong \omega_s + \omega_z \delta_z \sin(\omega_z t + \beta_z) \quad (3.8)$$

where

$$\omega_s = \omega_d - \omega_{hp} E \langle \cos 2\xi \rangle \quad (3.9)$$

It is necessary to include the correction of equation (3.9) because phase-locking demands that $\omega_{hp}^2 E^2 > \omega_d^2$. However all time-varying components of $\omega_{hp} E \cos 2\xi$ are negligible compared to $\omega_z \delta_z \sin(\omega_z t + \beta_z)$.

Equation (3.8) is readily integrated.

$$\xi = \omega_s t + \xi_0 - \delta_z \cos(\omega_z t + \beta_z) \quad (3.10)$$

Now, to evaluate $\langle \sin 2 \xi \rangle$, it is necessary to expand $\sin 2 \xi$ in terms of an infinite number of single frequency components.

$$\sin 2 \xi = J_0(2 \delta_z) \sin 2 x \quad (3.11)$$

$$+ \sum_{n=1}^{\infty} (-1)^n J_{2n}(2 \delta_z) \left\{ \sin 2 [x + ny] + \sin 2 [x - ny] \right\}$$

$$- \sum_{n=0}^{\infty} (-1)^n J_{2n+1}(2 \delta_z) \left\{ \cos [2x + (2n + 1)y] \right.$$

$$\left. + \cos [2x - (2n + 1)y] \right\}$$

where $x = \omega_s t + \xi_0$

$$y = \omega_z t + \beta_z$$

$$J_p(2 \delta_z) = \text{Bessel function of the first kind.}$$

The time average value of $\sin 2 \xi$ is immediately evident provided the averaging time is sufficiently long. This latter point is taken up in part C of this section.

$$\langle \sin 2 \xi \rangle = -J_m(2 \delta_z) \quad (3.12)$$

$$\text{for } \omega_s = \pm m \frac{\omega_z}{2}$$

$$\text{where } m = 0, 1, 2, 3,$$

The phase ξ_0 is selected to give $\langle \sin 2 \xi \rangle$ its maximum negative value.

Under the conditions of equation (3.12), $\langle \cos 2\xi \rangle = 0$ and so $\omega_s = \omega_d$.

Finally, the threshold is computed from equation (2.38).

$$\omega_{h' \text{ crit}} = \text{Min} \left\{ \frac{\omega_{\ell k}}{E J_m(2\delta_z)} \right\} \quad (3.13)$$

This threshold can be rewritten in terms of the threshold without modulation, equation (2.45).

$$\boxed{\frac{h'}{h_c} = \text{Min} \left\{ \frac{1}{J_m(2\delta_z)} \right\}} \quad (3.14)$$

It is understood that the particular sideband excited is determined by that value of m which gives the lowest threshold in equation (3.14). The resulting curve of the increase in threshold vs. δ_z is shown in Figure 3-2. Data is taken from standard tables.¹⁹ For convenience in taking experimental data this same curve is replotted in Figure 3-3 with the level of suppression given in decibels. Two interesting features have been observed.

First note that the curve rapidly levels off in Figure 3-3. It has been found, graphically, that for $2\delta_z = 56$, only 15 db of suppression can be attained; that is, a law of diminishing returns appears evident. Secondly, it has been observed that, at least for $1.83 \leq 2\delta_z \leq 56$, a curve, described by equation (3.15) can be fitted to the minima of each of the lobes of Figure 3-2.

$$20 \log_{10} \left(\frac{h'}{h_c} \right) = 7 \log_{10} (5\delta_z) \quad (3.15)$$

Equation (3.15) has been drawn in on Figure 3-3. This equation predicts that

for $2 \delta_z = 1000.$, $h'/hc = 15.46$ or 23.8 db.

Finally, a comment is in order on the modulation parameter, δ_z , given with equation (3.5).

$$\delta_z = \frac{\omega_k (1 + \epsilon^2) \omega_{hz}}{\epsilon \omega_p \omega_z} \quad (3.16)$$

In the parallel pumping experiment $\omega_p \approx 2 \omega_k$ and is fixed. The value of the ellipticity, ϵ , is a function of the point of operation of the butterfly curve, Figure 2-4b. ϵ is fixed and a minimum in the range $H \leq H_c$. From $H = H_c$ to $H = H_d$, ϵ increases to 1. It would be interesting to measure the effect of ϵ on the modulation parameter; however, for a pumping frequency of 9.2 Gc. the minimum value of ϵ ($= .5945$ in YIG) is not sufficiently small to produce a noticeable effect on δ_z ($\frac{1 + \epsilon^2}{2\epsilon} = 1.138$). Experiments at much lower frequencies are necessary to confirm the predicted behavior in equation (3.16).

B. Experimental results

Observations have been made on a 100.0 mil diameter sphere of pure Yttrium Iron Garnet (YIG). The pump frequency was 9043. megacycles and the sample was biased to the corner of the butterfly curve ($H_c = 1590$ o e.) (see Figure 2-4b). This point is chosen simply because the r. f. magnetic field needed for instability is least. At this point the r. f. magnetic field at threshold was calculated to be $hc = 0.25$ o e. This implies a spin wave full linewidth of $2 \Delta H_{ko} = 0.14$ o e., or in terms of frequency, $2 \omega_{lk} = 0.386$ mc.

The necessary fields have been achieved in the cavity-coil configuration of Figure 3-4. By employing a circular coil of the proper diameter in a

T E₀₂₁^o mode cavity, it has been possible to provide parallel fields of adequate strength with no interaction between the circuitry of the two longitudinal fields. Details of the cavity, the coil and the modulation circuit are given in Appendices III-A and III-B.

Spin wave instabilities have been observed through the reflection coefficient of the T E₀₂₁ cavity. A block diagram of the necessary microwave circuit is shown in Figure 3-5. The basic features include frequency stability to better than one part in 10⁸, power capability to 5 watts, incident, and a pulse rise time of less than one-half microsecond. Relative power levels are determined by the setting of a precision variable attenuator (P. V. A.). The applied magnetic field is monitored with a Hall Effect Gaussmeter. A discussion of the microwave circuit and its associated problems is given in Appendix III-C.

Measurements were made for several different modulating frequencies as shown in Figures 3-6 and 3-7. In each case the data is compared with the curve of Figure 3-3. Because of a small uncertainty in the absolute value of h_z , a correction factor of 1.37 has been applied to the approximate calibration of Appendix III-B in calculating h_z . This correction factor was determined by fitting data to the theoretical curve at $f_m = 3.55$ mc. The same factor has been applied at all lower frequencies.

Minor disagreement at discrete points may be noted in Figure 3-6. This error is attributed to the problem of recognizing the threshold. More important, it is to be noted that the degree of suppression becomes increasingly less than suggested by the theory as the suppression frequency decreases. This is noticeable for $f_m \leq 1.52$ mc. The same effect has been observed¹⁷ for the analogous experiment in which the pump frequency is modulated to suppress the instability threshold. It is apparent that this

breakdown occurs when the modulating frequency becomes of the same order of magnitude or less than the relaxation frequency of the spin waves ($2 \omega_{\ell k} = 0.386 \text{ mc.}$). This is to be expected, physically, because the spin waves are able, to a certain extent, to follow the modulating field. A possible theoretical derivation is discussed in the next section.

C. Low frequency modulation

In part A of this section it was tacitly assumed that the modulation frequency, ω_z , is relatively high compared to the relaxation frequency of the spin waves, $\omega_{\ell k}$. Thus, over the period of time required for buildup of instability, the average value of $\sin 2 \xi$ is that of very many periods, i. e. the steady-state average. However, as ω_z becomes comparable to or less than $\omega_{\ell k}$, it is apparent that the averaging process must be altered. Equation (2. 38) becomes:

$$\omega_{\text{crit}} = - \frac{\omega_{\ell k}}{E \langle \sin 2 \xi \rangle_T} \quad (3. 20)$$

where the time average is taken over a finite period of time, T , as yet indeterminate. This same argument applies whether the excitation is pulsed or continuous. As the "bias" (d. c. field plus modulation) sweeps back and forth, each spin wave excited has associated with it a finite buildup time. For a narrow band of spin waves, it is assumed that this time is the same for all.

As an example of the finite time averaging process consider the excitation of the center frequency spin waves ($\omega_s = 0$, $\omega_d = 0$, $\cos 2 \xi_0 = 0$).

$$- \langle \sin 2 \xi \rangle_T = \langle \cos [2 \delta_z \cos (\omega_z t + \beta_z)] \rangle_T \quad (3. 21)$$

It can be expected that the lowest threshold is to be observed as the bias passes through the limits of its swing [$\sin(\omega_z t + \beta_z) = \pm 1$]. Therefore, an average is considered over either of two intervals.

$$\frac{\pi}{2} - \frac{\omega_z T}{2} < (\omega_z t + \beta_z) < \frac{\pi}{2} + \frac{\omega_z T}{2} \quad (3.22)$$

or

$$-\frac{\pi}{2} - \frac{\omega_z T}{2} < (\omega_z t + \beta_z) < -\frac{\pi}{2} + \frac{\omega_z T}{2} \quad (3.23)$$

In both cases the desired time average is the same.

$$\langle \cos [2 \delta_z \cos(\omega_z t + \beta_z)] \rangle_T, \max = \quad (3.24)$$

$$J_0(2 \delta_z) + 2 \sum_{n=1}^{\infty} J_{2n}(2 \delta) \left(\frac{\sin n \omega_z T}{n \omega_z T} \right)$$

This expression has the desired features. For $\omega_z T$ very large it equals $J_0(2 \delta_z)$ as expected for a long time average. As $\omega_z T$ decreases, the center frequency term, $J_0(2 \delta_z)$, is enhanced by the sideband terms, $J_{2n}(2 \delta_z)$, as shown in Figure 3-8. This is in keeping with a suggestion in the literature that, for low modulation frequencies, the sidebands overlap. As $\omega_z T$ approaches zero the right hand side of equation (3.24) becomes unity for all δ_z . Qualitatively, this behavior is in good agreement with experimental observations. 17, 18

The present apparatus does not allow for a study at very low modulation frequencies; therefore, it is as yet not possible to compare the curves of Figure 3-8 with experimental data and, thus, to compute the time, T, if indeed it has a valid definition.

Although the exact behavior of equation (3.5) has been ignored, the quantity $\omega_z \delta_z$ does remain large wherever a measureable degree of suppression is evident.¹⁷ Physically, this mathematical description is appealing in that it describes the overall effect of excitation as the modulation swings back and forth at low frequencies. In this way, interactions between spin waves can be ignored and the observation of instability is tied directly to the time average growth of a single amplitude, A. Thus, it is expected that equation (3.24) is a good description of the first lobe of the suppression curve as a function of modulation frequency.

APPENDIX III - A

THE TE₀₂₁⁰ CAVITY

This cavity has been designed to provide efficient coupling to the sample at both the microwave and the modulating frequencies. A single turn coil has been placed at midlength inside the cavity at a position where its coupling to the microwave field is negligible. This avoids the necessity of penetrating the cavity wall with a low frequency signal. The sample is located at the geometric center of the cavity. Dimensions are given in Figure 3.9.

The field pattern of the TE₀₂₁⁰ mode in a circular cylindrical cavity is described below and shown schematically in Figure 3.10.

$$\underline{h}_r = +h_o \left(\frac{\pi}{2X_{02}} \right) P J_o' \left(X_{02} r/a \right) \cos \left(\frac{\pi z}{d} \right) \quad (3.30)$$

$$\underline{h}_z = +h_o J_o \left(X_{02} r/a \right) \sin \left(\frac{\pi z}{d} \right)$$

$$\underline{e}_\phi = +j h_o \left(\frac{a \mu_o \omega}{X_{02}} \right) J_o' \left(X_{02} r/a \right) \sin \left(\frac{\pi z}{d} \right)$$

$$\underline{h}_\phi = \underline{e}_r = \underline{e}_z = 0$$

where h_o = r.f. magnetic field amplitude at the geometric center

$$X_{02} = \text{second zero of } J_o'(X) = 7.016$$

$$P = 2 a/d$$

d = length of cavity

a = radius of cavity

$J_o(X)$ = zero order Bessel function.

Note that at $r = \left(\frac{X_{01}}{X_{02}} \right) a = (0.5462) a$, $\underline{e}_\phi = 0$. A circular loop of this radius does not couple to the microwave fields. However, the dielectric support for the coil

causes a frequency shift and drop in Q because it lies in the plane of the e - field. In the present cavity, the unloaded Q of the empty cavity is measured to be 6×10^4 at a resonant frequency of 9186 mc. With the coil and coil form in place the cavity characteristics are as given below.

$$f_o = 9043. \text{ mc.}$$

$$Q_o = 6700.$$

$$\beta_o = 0.6457$$

$$Q_{1o} = 4348.$$

$$h_o^2 / P_{ic} = 2.792 \text{ oe}^2/\text{watt}$$

The last term indicates the r.f. magnetic field expected for a given amount of incident power.

All TE_{onl}^o modes are degenerate with TM_{1nl} modes. In the present case the TM_{121}^o mode is suppressed by a slot cut in the cavity end wall. The surface currents of the TM_{121}^o are interrupted but not those of the TE_{021} .

APPENDIX III - B

THE COIL AND MODULATION CIRCUIT

The single turn coil employed exhibits a very low impedance with fairly high Q. The equivalent series inductance and resistance have been measured on a Q-Meter as:

$$L = 0.128 \mu H$$

$$R = 0.01 \Omega$$

In order to match this coil to a transmission line it is necessary to bring it to resonance with an external capacitor. The field is then measured indirectly through the voltage developed across the coil terminals. The field is computed to be:

$$h_z = \frac{0.508 V_{rms}}{f_z (mc.)} \quad (3.31)$$

where h_z = field strength at the center and in the plane of the loop.

V_{rms} = r. m. s. voltage measured across the coil terminals.

f_z = frequency of excitation in megacycles.

By means of a search coil, this expression was found to be correct within a factor of 1.5 .

Actual field strength measurements were corrected as mentioned in Section III. 2 B.

The coupling and monitoring circuit used in the parallel pump experiment is shown in Figure 3. 11. It was designed and built to cover the modulating frequency range of 0.3 to 3.5 mc. Because of severe loading on the signal source at the low frequencies, it is necessary to monitor and adjust the frequency as the generator output is altered.

APPENDIX III - C

THE MICROWAVE CIRCUIT

The circuit used to observe parallel pump instability is shown in Fig. 3.12. The measurement depends upon observation of the reflection coefficient, Γ , of the cavity as a function of time. With the cavity driven at its resonant frequency Γ is given by equation (3-38) from Appendix III-D.

$$\Gamma = \frac{\Gamma_o + \eta Q_{LO} \chi''}{1 + \eta Q_{LO} \chi''} \quad (3-38)$$

where Γ_o = reflection coefficient without magnetic loss

η = filling factor

Q_{LO} = loaded Q of cavity without magnetic loss

χ'' = imaginary component of susceptibility used to describe magnetic loss

In the parallel pump experiment, the reactive component of susceptibility is negligible.

The important features of the circuit are stability of frequency and power level, measurement of absolute incident power level, and sensitivity of the detection system. The frequency of the source must be stable, both long and short term, to a fraction of the bandwidth of the sample cavity. Variation of the frequency of the source leads to large amplitude variation in the reflected power because of the high Q and the near unity coupling coefficient of the cavity. The instability threshold is then difficult to detect. Drift in the source can cause considerable error primarily because the field strength at the sample is determined by the cavity reflection coefficient at the excitation frequency (see equation 3-42). The use of a crystal controlled stabilizer reduced these

problems to a small magnitude.

To observe instabilities as a function of power level, it is necessary that the r.f. power level be constant in time to better than 0.1 db. In this regard, it was sufficient to employ a klystron to drive a TWT amplifier, both with well regulated power supplies. To obtain pulses of r.f., a diode switch is employed between klystron and TWT. Thus, it is possible to turn on and off the r.f. without introducing frequency modulation. A waveguide switch is provided to bypass the TWT when desirable. The precision variable attenuator (P.V.A.) allows one to set the relative power level to an accuracy of 0.1 db.

To measure the power incident on the cavity an arrangement has been employed which permits said power to be switched to a thermistor head.

The reflected power from the cavity is detected by a sequence law crystal, amplified by a low noise preamplifier (Adage Ultra-Null ND-2), and displayed on an oscilloscope as a means of detecting changes in the cavity reflection coefficient.

APPENDIX III - D

Useful Relations from Perturbation Theory

In this appendix, it is assumed that the real component of susceptibility, $\chi = \chi' - j \chi''$, is zero, $\chi' = 0$, for a ferrimagnetic sample under observation in a one-port cavity. This is always true for all practical purposes in the parallel pumping experiment. It is also true when observation is made of the saturation of the main resonance excited at its resonant frequency.

A well known result from perturbation theory for a sample in a uniform field is given in equation (3.32).²⁰

$$\frac{1}{Q_1} = \frac{1}{Q_{10}} + \eta \chi'' \quad (3.32)$$

where Q_{10} = unperturbed loaded Q

Q_1 = perturbed loaded Q

η = Filling factor = $\frac{V_s}{2gV_c}$

V_s = Sample volume

V = cavity volume

g = $\frac{W}{\mu_0 h_0^2 V_c}$

W = total stored energy in unperturbed cavity

h_0 = magnetic field amplitude at sample

In the following formulae the subscript o denotes the unperturbed state.

In general the loaded, unloaded and external Q of a cavity are interrelated with a coupling coefficient, β .

$$Q_{10} = \frac{Q_0}{\beta_0 + 1} \quad Q_1 = \frac{Q}{\beta + 1} \quad (3.33)$$

$$Q_x = \frac{Q_0}{\beta_0} = \frac{Q}{\beta} \quad (3.34)$$

where Q, Q_0 are the unloaded Q's

$$Q_x = \text{external } Q.$$

In general one can write for the coupling coefficient, β :

$$\beta = \frac{\beta_0}{1 + \eta Q_0 \chi''} \quad (3.35)$$

The reflection coefficient, Γ , of the cavity excited at its resonant frequency is:

$$\Gamma = Q_1 \left(\frac{1}{Q} - \frac{1}{Q_x} \right) \quad (3.36)$$

$$= \frac{1 - \beta}{1 + \beta} \quad (3.37)$$

$$\Gamma = \frac{\Gamma_0 + \eta Q_{10} \chi''}{1 + \eta Q_{10} \chi''} \quad (3.38)$$

where

$$\Gamma_0 = Q_{10} \left(\frac{1}{Q_0} - \frac{1}{Q_x} \right) = \frac{1 - \beta_0}{1 + \beta_0}$$

All of the above formulae apply whether the cavity is over or undercoupled.

The unloaded Q of the unperturbed cavity can be written in terms of the total stored energy and the power dissipated in the cavity:

$$Q = \frac{\omega_o W}{P_d} \quad (3.39)$$

where

$$P_d = (1 - |\Gamma|^2) P_{ic} \quad (3.40)$$

where P_{ic} = incident power

and

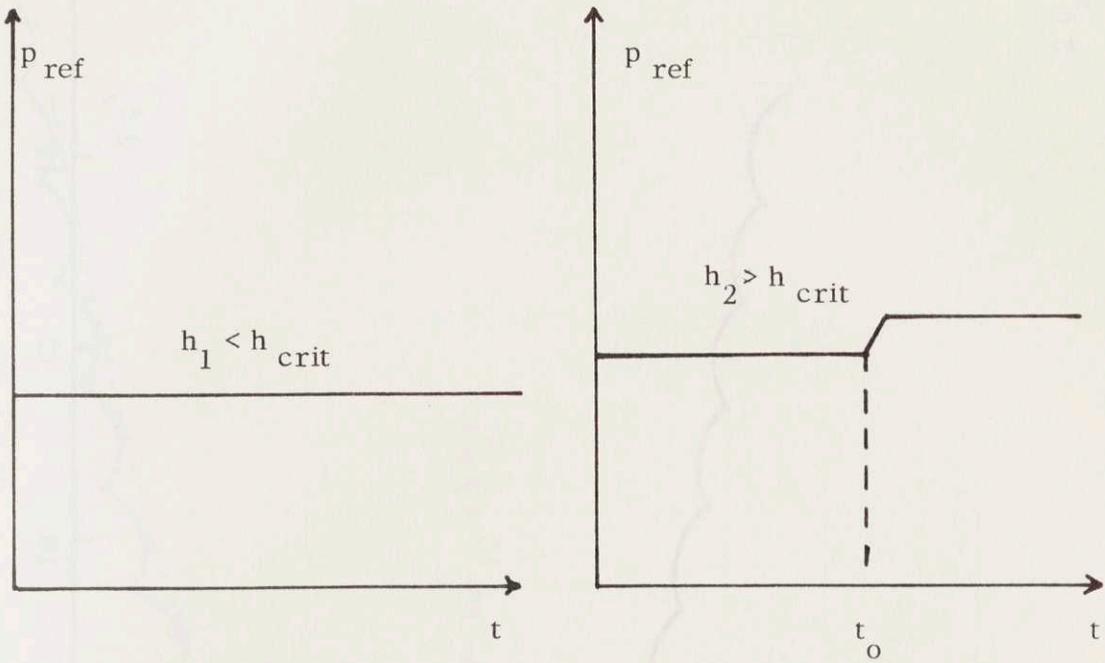
$$W = \mu_o h^2 g V_c \quad (3.41)$$

Thus, the r. f. magnetic field in an unperturbed cavity at resonance is given by

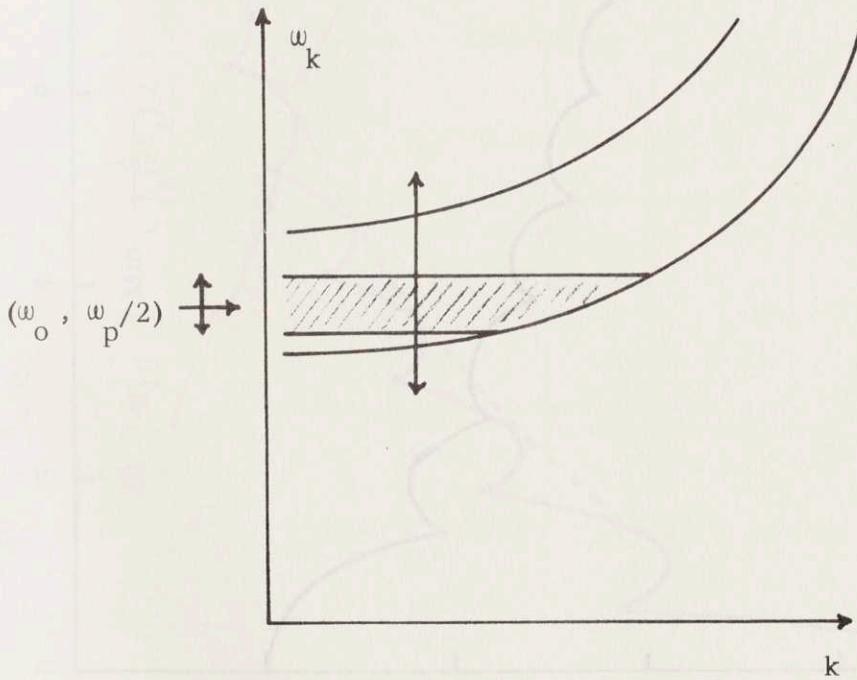
$$\frac{h_o^2}{P_{ic}} = \frac{Q_o (1 - \Gamma_o^2)}{\omega_o \mu_o g V_c} \quad (3.42)$$

and in a perturbed cavity at resonance by

$$h = \frac{h_o}{1 + \eta Q_{lo} \chi''} \quad (3.43)$$



a) Reflected Power below and above threshold



b) Spread of Excitation by Modulation

FIGURE 3.1

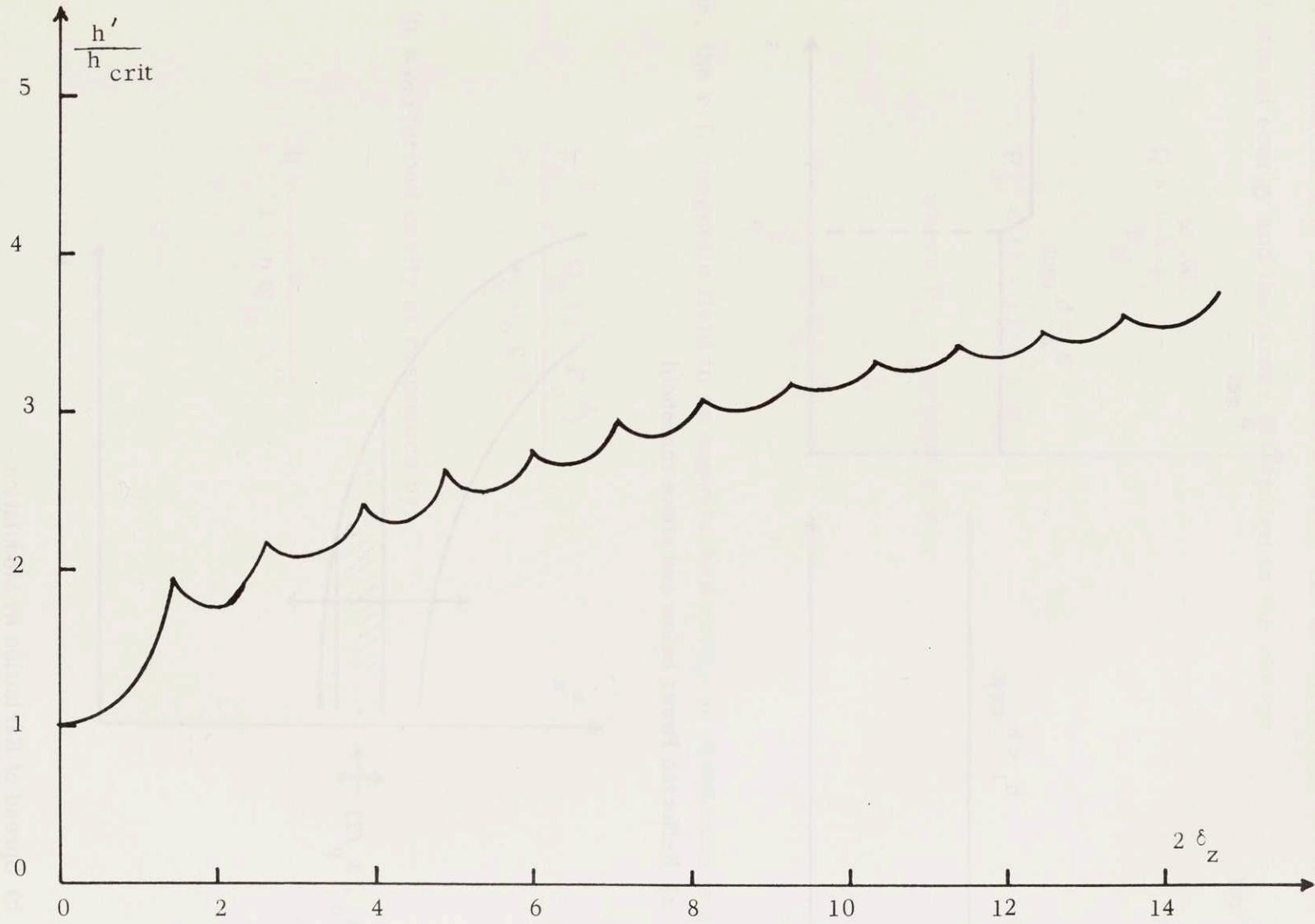


FIGURE 3.2 Parallel Pump Suppression Curve

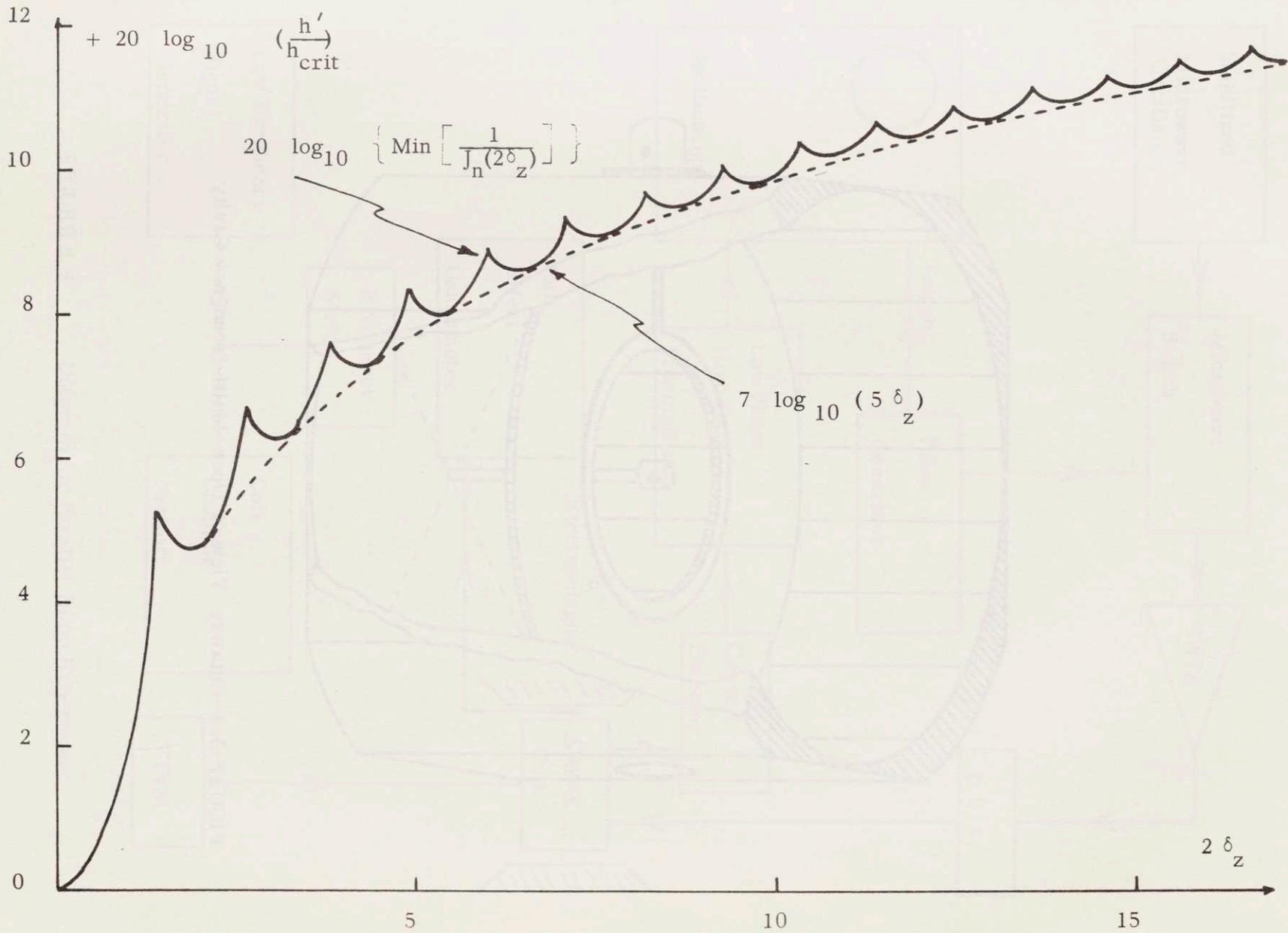


FIGURE 3.3

Suppression in DB.

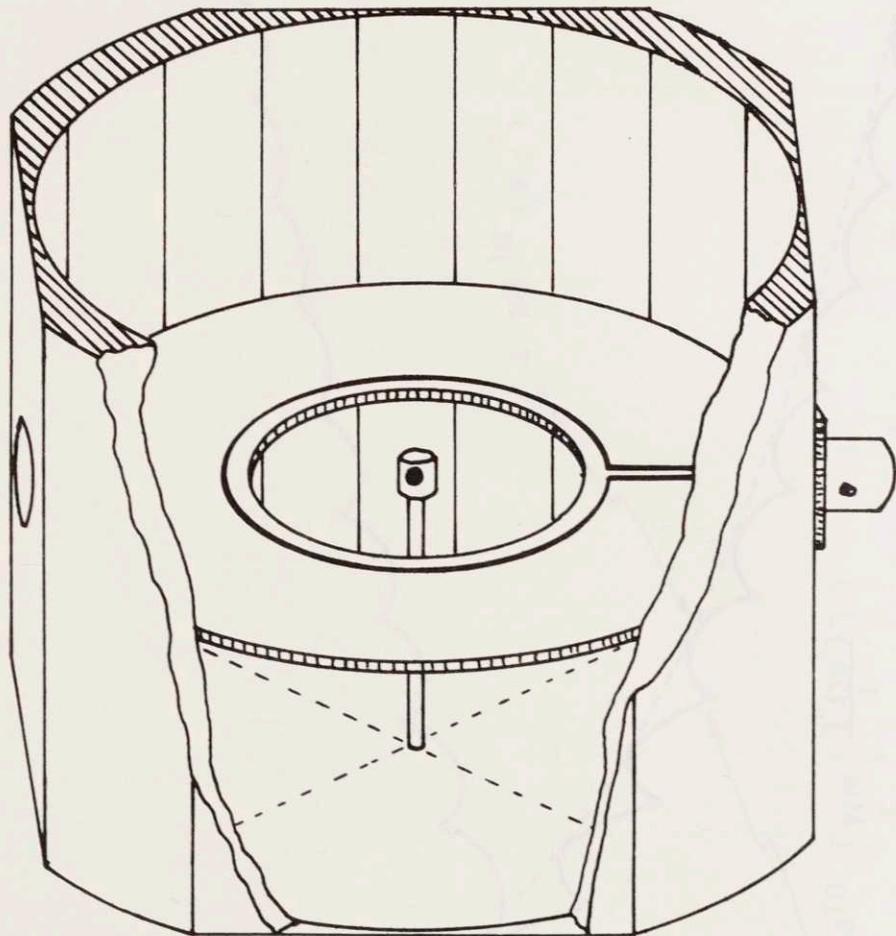


FIGURE 3.4 Cutaway View of Open Multi-frequency Cavity

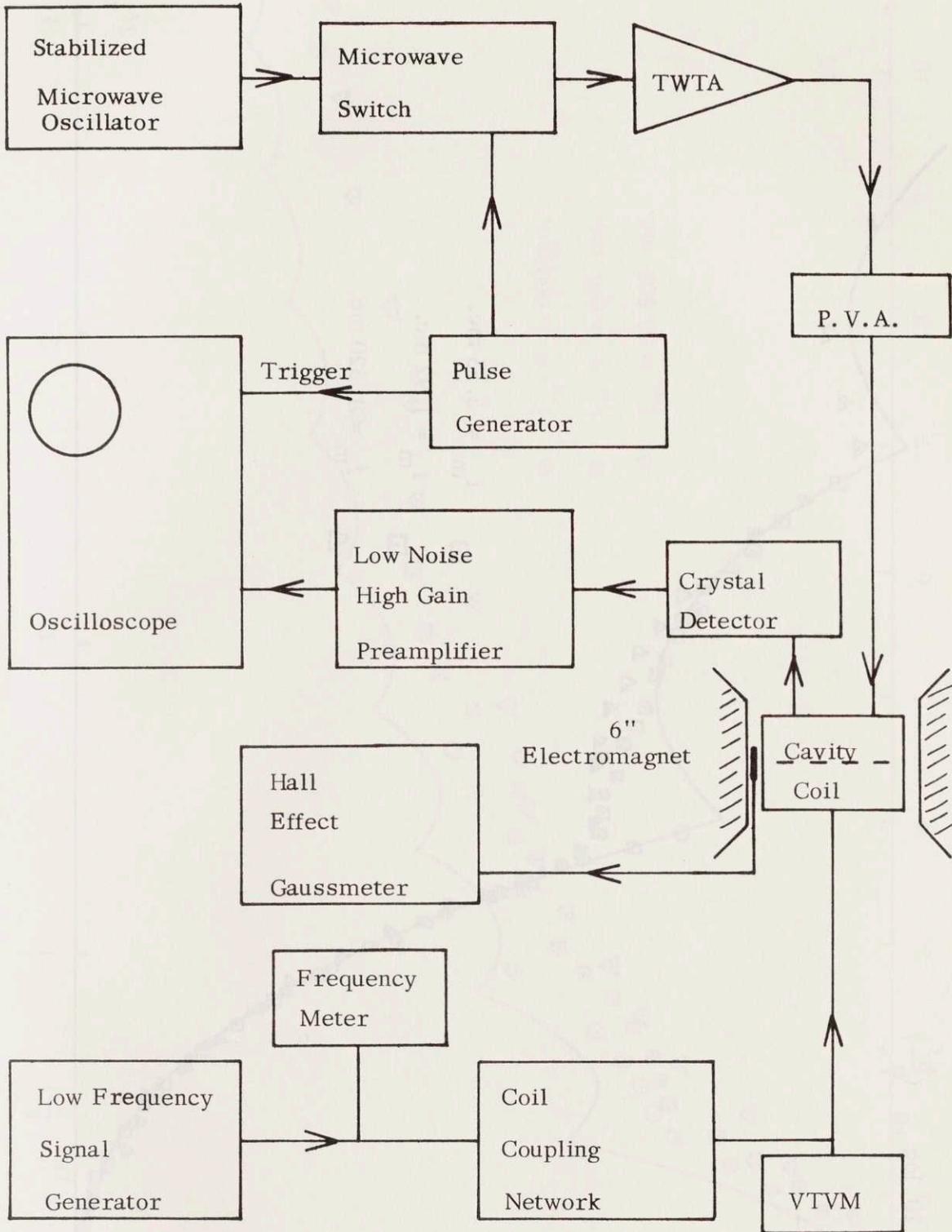


FIGURE 3.5 Diagram for Parallel Pump Experiment

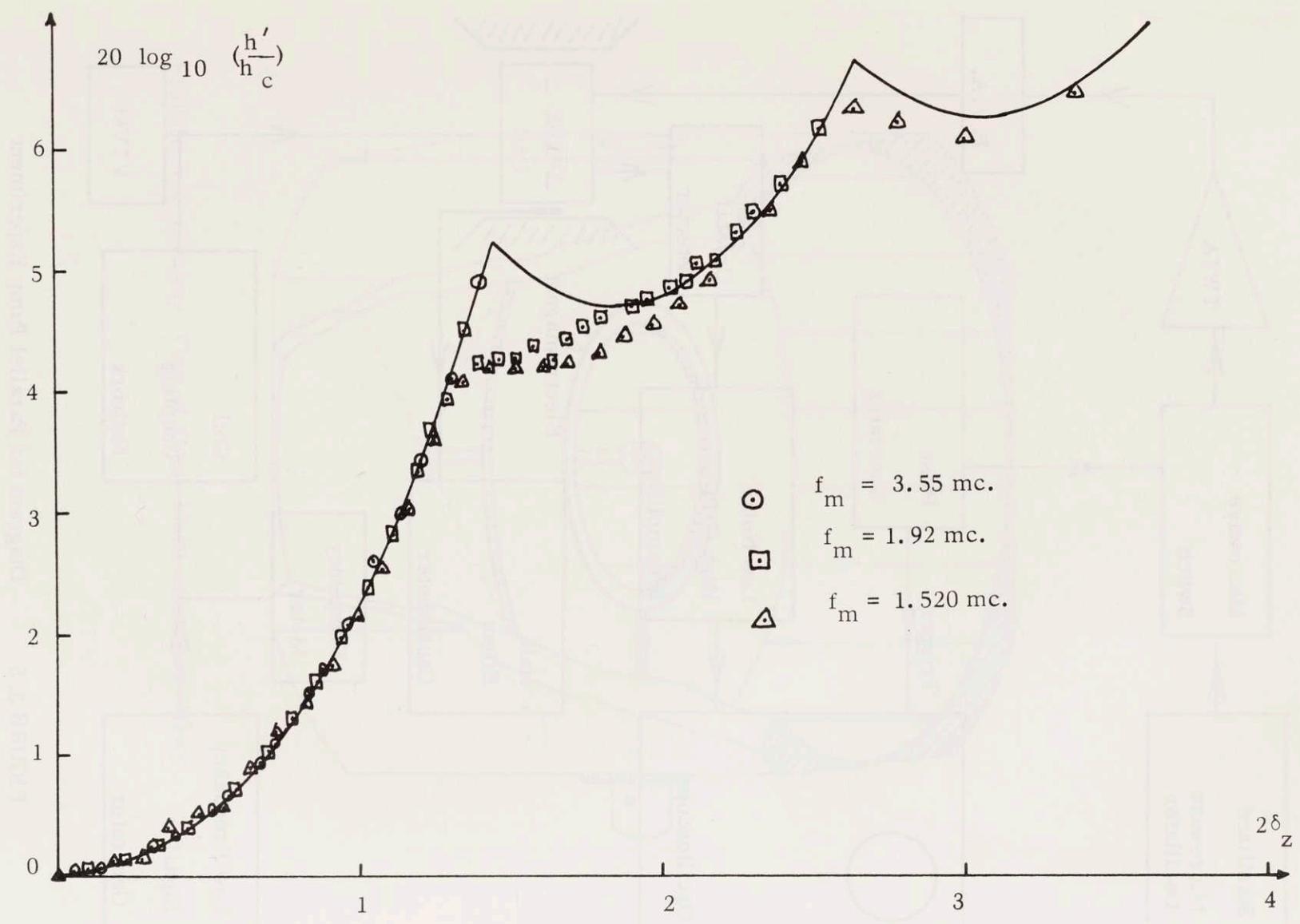


FIGURE 3.6 Parallel Pump Suppression $\omega_z \gg \omega_{\ell k}$

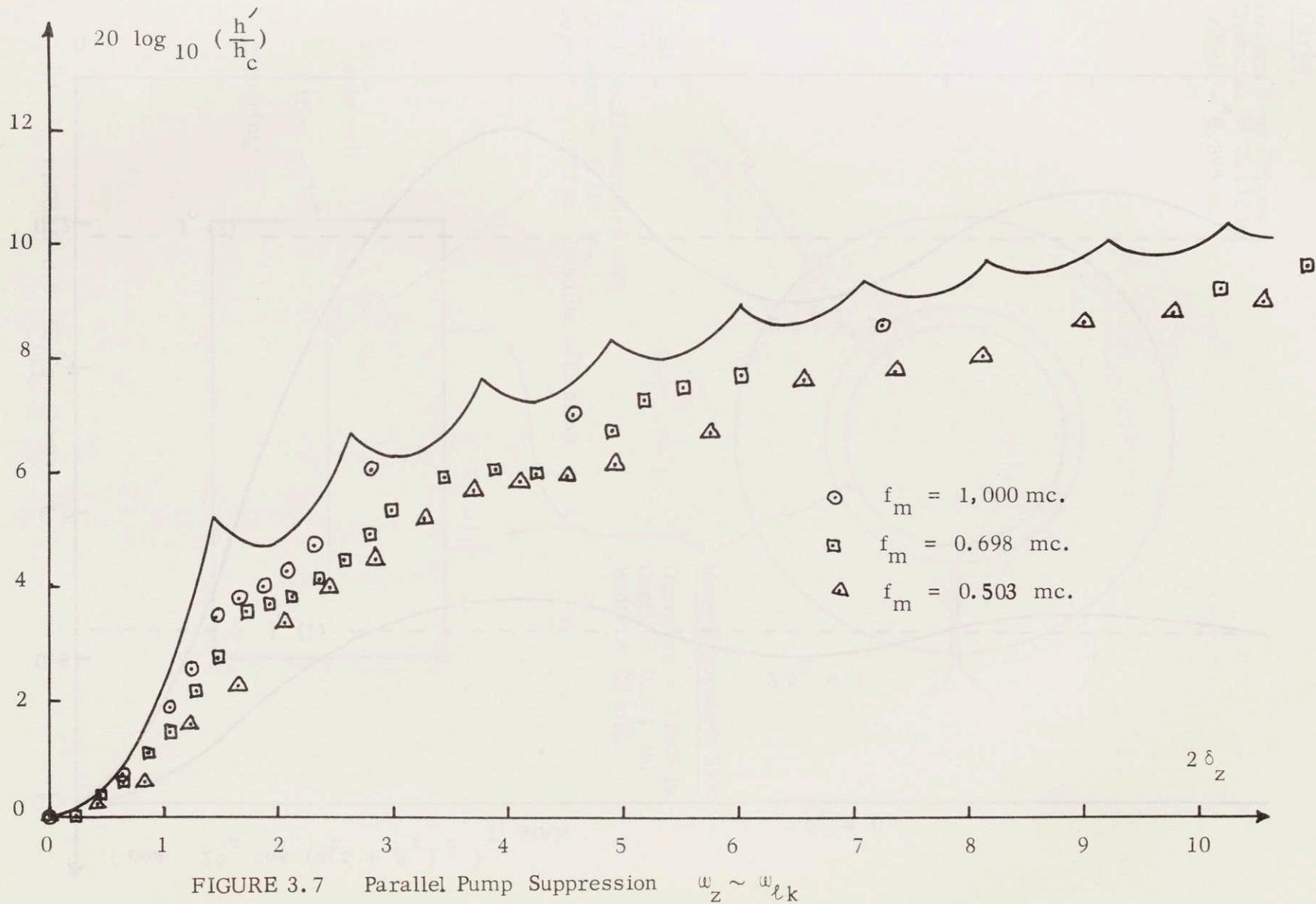


FIGURE 3.7 Parallel Pump Suppression $\omega_z \sim \omega_{lk}$

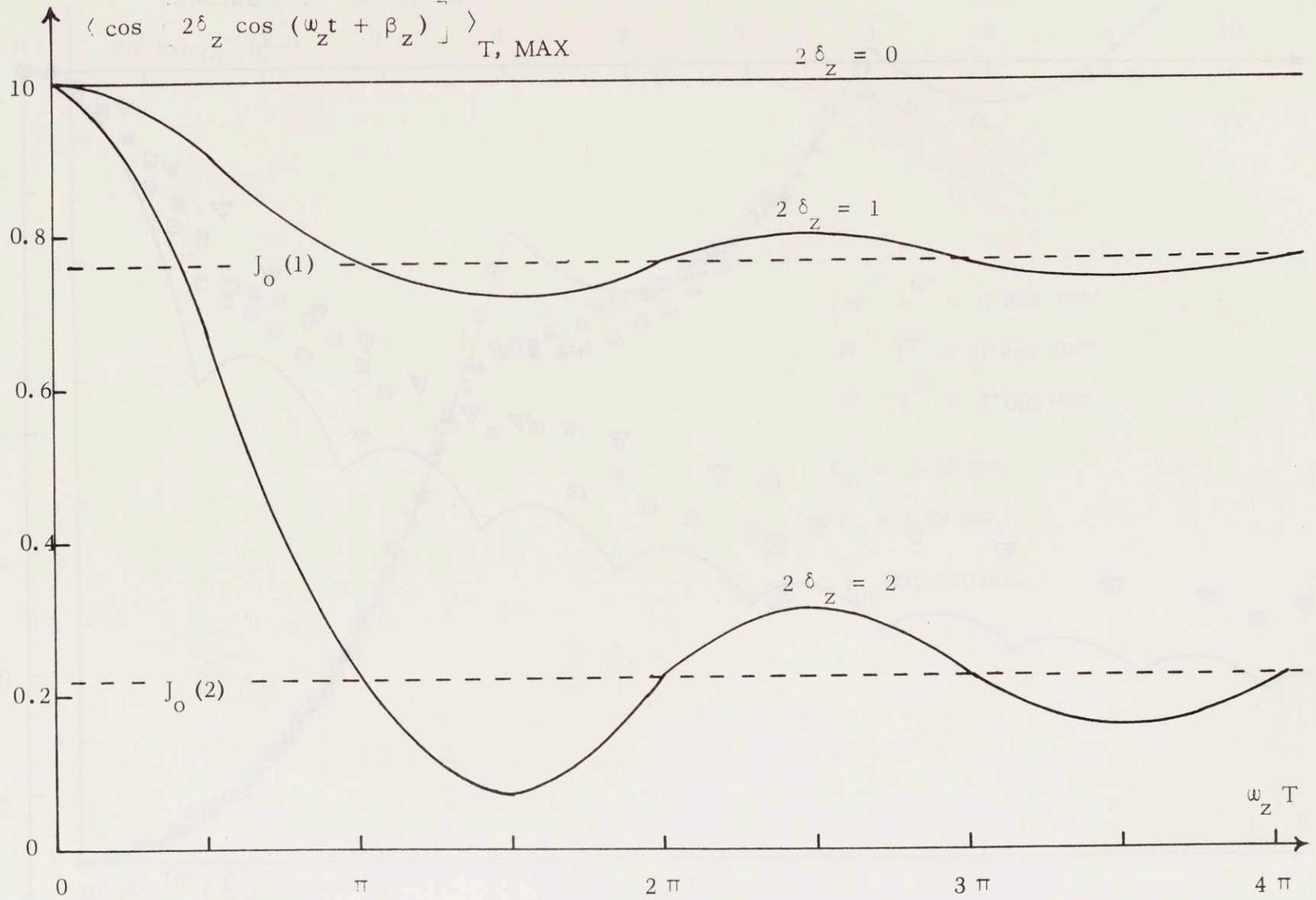


FIGURE 3.8 "Finite Time" Average

Cavity

Oxygen Free Copper
Diameter = 3.132 in.
Length = 1.595 in.

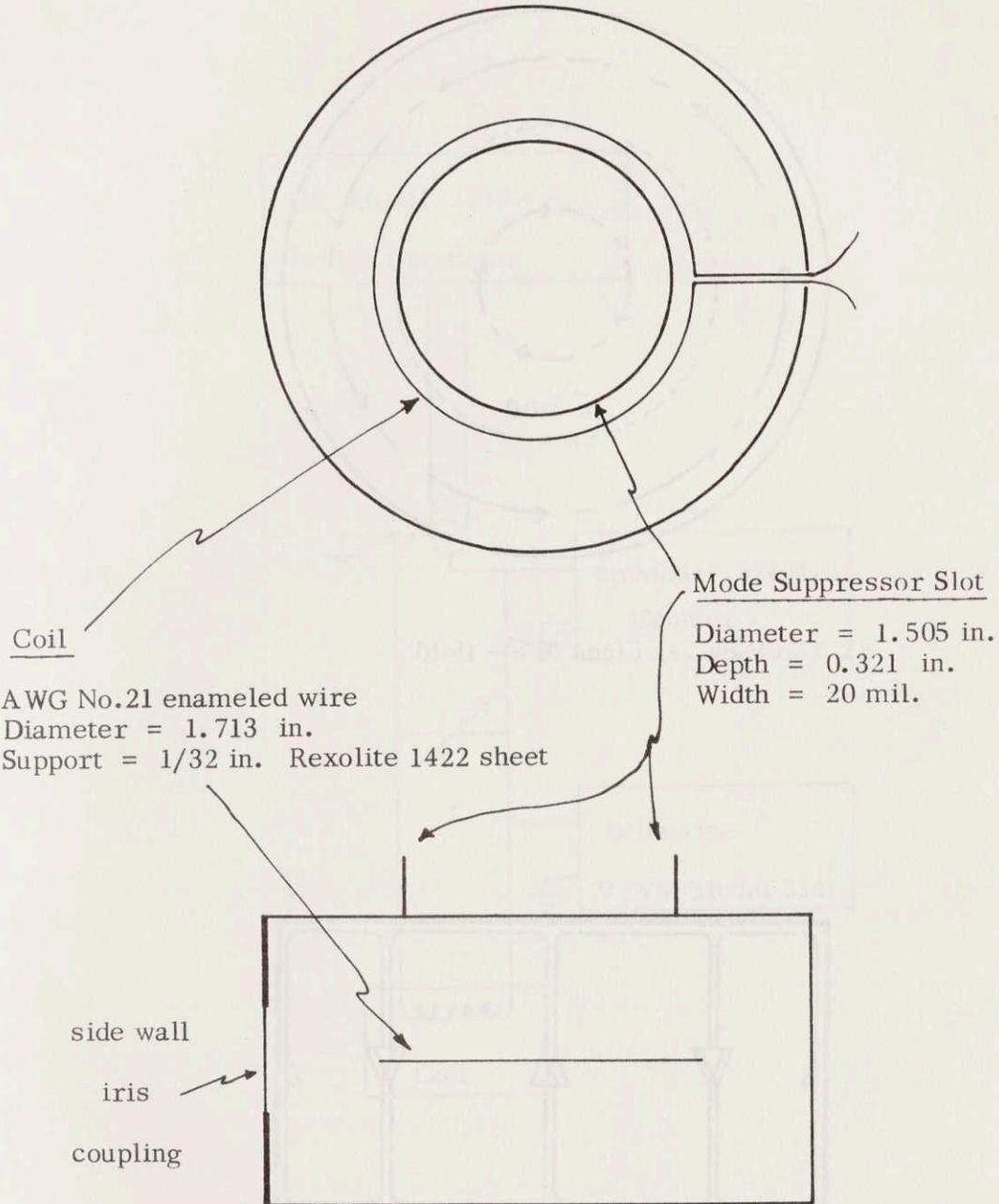
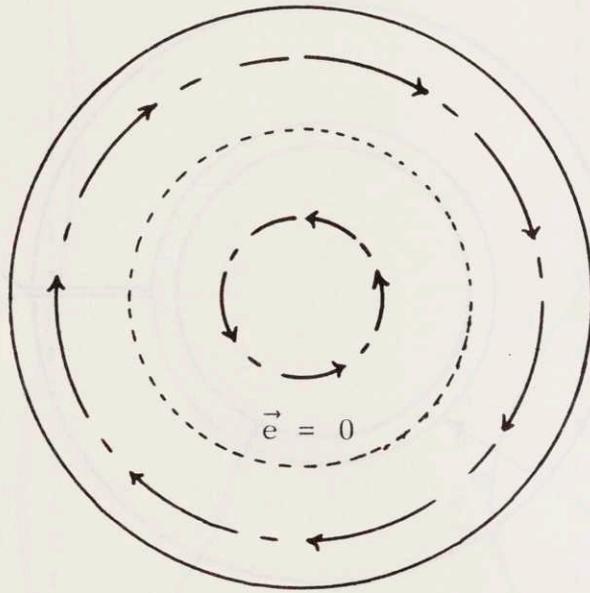
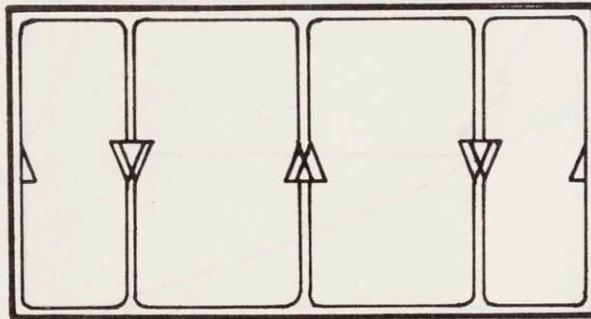


FIGURE 3.9 TE_{021}^0 Cavity



a) Top View - Lines of \vec{e} - field



b) Cross Section View - Lines of \vec{h} - field

FIGURE 3.10

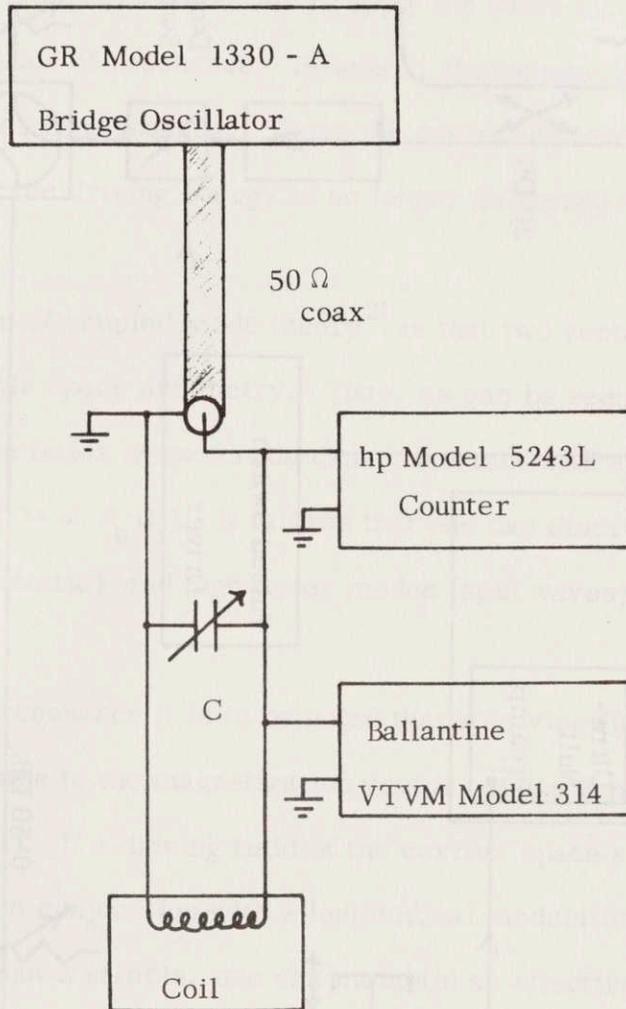


FIGURE 3.11 Modulation Circuit

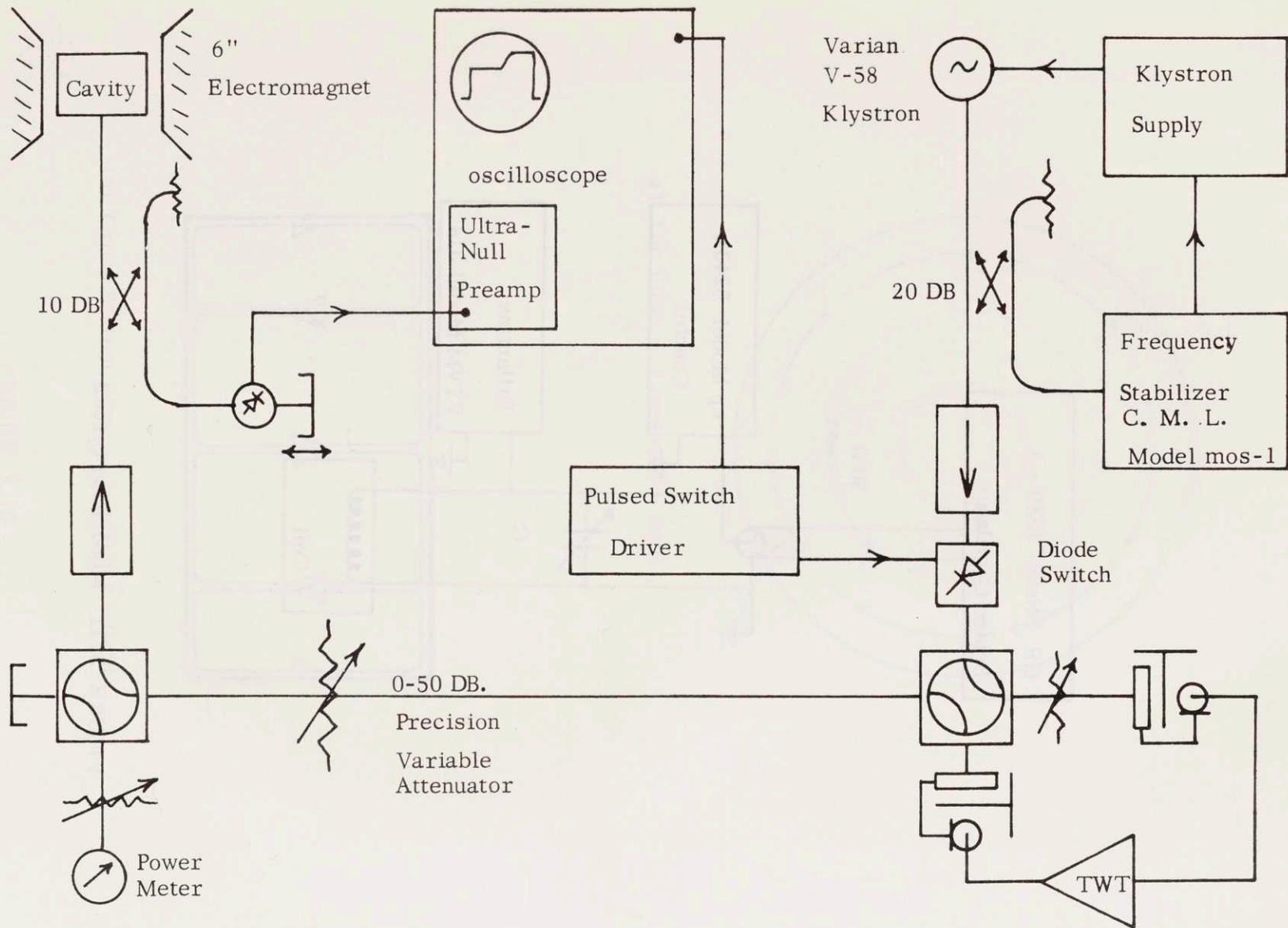


FIGURE 3.12 Circuit Diagram for Parallel Pumping.

CHAPTER IV

STABILIZATION OF THE MAIN RESONANCE

IV.1 A physical picture

Since it has been demonstrated that an instability threshold can be raised significantly by field modulation, it appears attractive to apply the same method to avoid saturation of the magnetostatic modes of resonance. However, the longitudinal modulation generates sidebands on all modes of resonance. Thus, the saturation level of a desirable mode may be increased but the driving energy is no longer delivered to just this one mode of response.

A useful principle of coupled mode theory²¹ is that two vector fields interact only if they have comparable space symmetry. Thus, as can be seen from equations (2.55) and (2.56), transverse fields of excitation cannot interact with a spin wave of high order spatial variation ($|\vec{k}| \gg \omega \epsilon_0 \mu_0$). It follows that one can discriminate between low order modes (magnetostatic) and high order modes (spin waves) in applying longitudinal modulation.

For any mode of resonance it is to be noted that a driving field-applied parallel at all times and in all space to the magnetization vector, \vec{M} , as it precesses - applies no torque (see Figure 4.1). If a driving field of the correct space symmetry and amplitude modulation is applied in conjunction with a longitudinal modulating field so as to produce this alignment throughout a sample, one can maintain an effective suppression field without the undesirable generation of sidebands.

In this chapter, attention is devoted to stabilization of the uniform precession in an isotropic spheroid biased along its axis of symmetry. First, the fields necessary to eliminate sidebands are discussed. Then, the extent to which the cone angle can be opened is derived. There follows a discussion of experimental conditions necessary to achieve the desired fields. Next, criteria for the recognition of proper operation are

developed from a discussion of experimental observations when the modulating fields are improperly aligned. Finally, a description of the system operating, as desired, and a curve of the spin wave suppression obtained, are presented.

IV. 2 Dual modulation of the uniform precession in an axially symmetric spheroid

A. Theory of the stabilized resonance

In the discussion of Section 1 and in Figure 4. 1, it has been shown that the modulating field will not generate sidebands if it precesses with and along the magnetization vector during ferromagnetic resonance. In general this configuration of fields and magnetization is not readily achieved; however, it can be in an isotropic sample with rotational symmetry about the applied d. c. field if driven at resonance by an amplitude modulated, circularly polarized, magnetic field of the form given in equations (4. 1 a, b, c).

$$h_z = -h \sin \omega_0 t + h \left(\frac{\omega_{h_z}}{\omega_{\ell_0}} \right) \sin (\omega_z t + \beta_z) \cos \omega_0 t \quad (4. 1a)$$

$$h_y = h \cos \omega_0 t + h \left(\frac{\omega_{h_z}}{\omega_{\ell_0}} \right) \sin (\omega_z t + \beta_z) \sin \omega_0 t \quad (4. 1b)$$

$$h_z = h_z \sin (\omega_z t + \beta_z) \quad (4. 1c)$$

When subject to this driving field, equations (2. 52) and (2. 53) become:

$$\dot{\varphi}_0 = \omega_0 - \frac{1}{\theta} \omega_h \cos (\omega_0 t - \varphi_0 + \frac{\pi}{2}) + \omega_{h_z} \sin (\omega_z t + \beta_z) \left[1 - \frac{1}{\theta} \frac{\omega_h}{\omega_{\ell_0}} \cos (\omega_0 t - \varphi_0) \right] \quad (4. 2)$$

$$\dot{\theta} = \omega_h \sin (\omega_0 t - \varphi_0 + \frac{\pi}{2}) - \omega_{\ell_0} \theta + \omega_{h_z} \frac{\omega_h}{\omega_{\ell_0}} \sin (\omega_z t + \beta_z) \sin (\omega_0 t - \varphi_0) \quad (4. 3)$$

As expected, the steady state solutions of (4. 2) and (4. 3) are the same as those with-

out modulation.

$$\varphi_0 = \omega_0 t \quad (4.4a)$$

$$\theta = \frac{\omega_h}{\omega_{L0}} \quad (4.4b)$$

Now consider the spin wave response with h_z given by (4.1) and φ_0 by (4.4a). Once again define $\Delta = \varphi_k - \varphi_0$. Equations (2.55) and (2.56) become:

$$\dot{\Delta} = (\omega_K + \omega_{KD} \theta^2 - \omega) + \omega_{KD} \theta^2 \cos 2\Delta + \omega_{h_z} \sin(\omega_z t + \beta_z) \quad (4.5)$$

and

$$\frac{\delta \dot{M}}{\delta M} = \theta^2 \omega_{KD} \sin 2\Delta - \omega_{Lk} \quad (4.6)$$

As in solving equation (3.5), assume $\omega_{h_z} \gg \omega_{KD} \theta^2 \geq \omega_{Lk}$, in which case:

$$\dot{\Delta} \approx \omega_s + \omega_{h_z} \sin(\omega_z t + \beta_z) \quad (4.7)$$

where

$$\omega_s = (\omega_K + \omega_{KD} \theta^2 - \omega) + \omega_{KD} \theta^2 \langle \cos 2\Delta \rangle \quad (4.8)$$

Once again, the alternating components of $\cos 2\Delta$ are assumed negligible compared to the modulation term.

Equation (4.7) is now integrated to give:

$$\Delta = \omega_s t + \Delta_0 - \frac{\delta'_z}{\omega_z} \cos(\omega_z t + \beta_z) \quad (4.9)$$

where

$$\delta'_z = \frac{\omega_{h_z}}{\omega_z}$$

The expansion of $\sin 2\Delta$ is exactly the same as that of $\sin 2\xi$ in equation (3.11). Here as in equation (3.12) it is assumed that ω_z is large compared with the spin wave relaxation frequency, ω_{Lk} . thus, an average is carried out over a long ($T \gg \frac{2\pi}{\omega_z}$) period of time.

$$\langle \sin 2\Delta \rangle = +J_m(2\delta'_z) \quad (4.10)$$

$$\text{for } \omega_s = \pm m \frac{\omega_z}{2}$$

where $m = 0, 1, 2, 3, \dots$

The phase Δ_0 has been selected so as to give $\langle \sin 2\Delta \rangle$ its maximum positive value.

Here $\langle \cos 2\Delta \rangle = 0$ and so $\omega_s = (\omega_K + \omega_{KD} \theta^2 - \omega)$. Finally the change in threshold is given by:

$$\frac{\theta'}{\theta_{\text{crit}}} = \sqrt{M \ln \left\{ \frac{1}{J_m(2\delta'_z)} \right\}} \quad (4.11)$$

Note in Figure 4.2 that in the present experiment a lesser degree of instability suppression is possible than in the parallel pump experiment. As in equation (3.15) a smooth curve can be fitted to Figure 4.2.

$$20 \log_{10} \left(\frac{\theta'}{\theta_{\text{crit}}} \right)^2 = 7 \log_{10} (5\delta'_z) \quad (4.12)$$

In alternate form:

$$\frac{\theta'}{\theta_{\text{crit}}} = (5\delta'_z)^{7/40} \quad (4.13)$$

Using equations (4.12) and (4.13) one can predict the behavior of equation (4.11) for large δ'_z .

$2\delta'_z$	$\theta'/\theta_{\text{crit}}$	$20 \log_{10}(\theta'/\theta_{\text{crit}})$
10	1.756	4.90 db
100	2.63	8.40 db
1000	3.93	11.90 db

B. Modulation of the transverse drive

In the present experiment, it is convenient to apply a field along just one rectangular coordinate axis as in equation (4.14).

$$h_y = 2h \cos \omega_0 t + 2h \left(\frac{\omega_z}{\omega} \right) \sin(\omega_z t + \beta_z) \sin \omega_0 t \quad (4.14)$$

This field consists of three sets of counterrotating circularly polarized fields at frequencies ω_0 , $\omega_0 \pm \omega_z$. The right-hand circularly polarized fields add up to give the fields of equations (4.1a, b, c). The left-hand circularly polarized fields, in effect, do not see a resonant mode and therefore may be neglected. This is generally true for a narrow linewidth material driven at resonance.

Because the coupling to a cavity is a function of frequency, the relative amplitudes of the carrier and modulated wave of equation (4.14) will be different in the wave incident on the cavity. However, the incident wave takes a similar form:

$$h(t) = h_a \left[\cos \omega_0 t + k_a \sin(\omega_z t + \beta_z) \sin \omega_0 t \right] \quad (4.15)$$

Because $\omega_z \ll \omega_0$, it is possible to describe this field in the complex domain as having a slow time-varying complex amplitude.

$$h(t) = \text{Re} \{ \underline{h}_a e^{j\omega t} \} \quad (4.16)$$

where

$$\underline{h}_a = [1 - jk \sin(\omega_z t + \beta_z)] h_a \quad (4.17)$$

This wave is composed of two parts: a carrier term with no modulation, and a term 90° out of phase with the carrier which consists of suppressed modulation. Such a wave can be produced by a combination of amplitude and phase modulation. A circuit capable of producing the desired modulation is shown in Figure 4-3. The E- and H-plane arms of a magic tee are terminated by a moveable short circuit on one and, on the other, an absorption modulator and short circuit capable of producing a time-varying reflection coefficient, $\Gamma = a(t)+b$. The short circuit produces a variable phase shift, ϕ relative to the phase of the variable reflection coefficient. For an incident wave, h_b , the output wave, h_a , is given by:

$$\underline{h}_a = \left\{ \left[1 - j \frac{a(t)}{\sin \phi} \right] - j \left[\frac{b + \cos \phi}{\sin \phi} \right] \right\} \frac{\underline{h}_b}{2} \sin \theta \quad (4.18)$$

By setting $b = -\cos \phi$ such that the $\sin \phi$ has a positive sign, the output is of the desired form.

Power in the output wave is of the form:

$$\frac{|\underline{h}_a|^2}{|\underline{h}_b|^2} = \frac{1}{4} \left\{ \left[a(t) + b + \cos \phi \right]^2 + \sin^2 \phi \right\} \quad (4.19)$$

With $a(t) = a \sin(\omega_z t + \beta_z)$, there are components of power transfer with frequencies $2\omega_z$ and ω_z . If and only if $b = -\cos \phi$, the ω_z term disappears. Thus, a square law detector can be utilized to align the modulator. Ambiguity in the sign of $\sin \phi$ can be resolved only by the proper operation of the system.

C. Experimental dual modulation

In order to make clear the alignment procedure for stabilization of the uniform precession, all possible interactions are discussed here in terms of the actual experiment. Four possible modes of operation are discussed in which either (1) longitudinal or (2) transverse modulation is applied separately, (3) the two are applied together but are not aligned, and finally (4) the modulation is completely aligned.

A system diagram is shown in Figure 4.4 . Basically, it is the same as in the parallel pump experiment with four modifications. The transverse modulator has been introduced between klystron and TWT. Second, the modulation system has provision for varying the amplitude and phase of the signal applied to the coil relative to that applied in the transverse modulator. Third the cavity has been modified for undercoupled excitation of the TM_{120}^0 mode (see Appendix IV-A). Fourth, detection is made with either a spectrum analyzer or the d. c. detection system of Appendix III-c as noted in the text.

In general, interactions within the sample are observed by reference to power reflected from the cavity at the center and sideband frequencies. However, detection of small changes in reflected power must be made using the d. c. detection system because of insufficient sensitivity of the spectrum analyzer to change in spectrum amplitude.

1. Longitudinal modulation only

Whereas modulation of the uniform precession has been studied for various applied waveforms,²³ no description is available in the literature for sinusoidal longitudinal modulation of the uniform precession. It is evident from the equation of motion, equation (2.5) That the uniform precession breaks up into an infinite set of sideband components as represented in equations (4.20) and (4.21).

$$m_x = \sum_n A_n \cos \left[(\omega_0 + n\omega_z) t + \alpha_n \right] \quad (4.20)$$

$$m_y = \sum_n B_n \sin \left[(\omega_0 + n\omega_z) t + \beta_n \right] \quad (4.21)$$

Solution for A_n , B_n , α_n , and β_n leads to an infinite determinant, the solution of which is beyond the scope of the present thesis. Even solution of a truncated problem in which just two sidebands are considered is algebraically tedious.

Assuming the above form of solution, it is evident that when driven by a linear field of the form:

$$h_y = 2h \cos \omega_0 t \quad (4.22)$$

there is to be expected power dissipation at the center frequency and power generation at the sidebands. The amplitude, h , in equation (4.22) is the actual field strength with the sample in place. That is, power dissipation at the center frequency is taken into account as in equation (3.43). The time average power dissipated (and scattered) is given by equation (4.23).

$$\langle P_D \rangle = \mu_0 \langle h_y \dot{m}_y \rangle = h B_0 \omega_0 \cos \beta_0 \quad (4.23)$$

Measurement of B_0 versus h_z is discussed in Appendix IV-C.

The power generated comes about through a reaction field²⁴ set up by the sideband components of \vec{m} . This field is linearly related to the magnetization at each frequency but its phase and amplitude are determined by cavity loading. The spectrum of power reflected from the cavity appears as shown in Figure 4.5a. The amplitude of sidebands is observed to diminish at frequencies far from the cavity resonant frequency because of frequency dependent coupling. Note that the reflected power at the center frequency is always decreased with the generation of sidebands.

2. Transverse modulation only

A transverse driving field of the form of equation (4.14) can be described in

terms of its frequency components as in equation (4.24).

$$h_y = 2h \cos \omega_0 t + h \left(\frac{\omega_{h_z}}{\omega_{\ell_0}} \right) \cos \left[(\omega_0 - \omega_z)t - \beta_z \right] - h \left(\frac{\omega_{h_z}}{\omega_{\ell_0}} \right) \cos \left[(\omega_0 + \omega_z)t + \beta_z \right] \quad (4.24)$$

With reference to the small signal equation of motion:

$$\dot{\vec{m}} = +\omega_0 (\vec{i} \times \vec{m}) - \omega_M (\vec{i}_z \times \vec{h}) \quad (4.25)$$

it should be noted that this equation is linear and, therefore, each of the sideband components in equation (4.26) can be treated independently. The resultant observation is that each component produces a reflected signal as if the others were not there (see Figure 4.5b). No other sidebands are observed.

3. Unaligned dual modulation

The interaction within the sample is the same as in subsection 1. above except that now there are three driving fields instead of two. The result is scattering of energy among the center frequency and two sideband fields as well as into the other sidebands.

4. Aligned dual modulation

Provided the relative amplitude and phase of the two modulation fields are correctly aligned, the magnetization exhibits no sidebands. Thus power is dissipated only at the center frequency, not at the sidebands. As shown in Figure 4.5c, one observes that the reflected power at the center frequency is the same as if no modulation were applied. The reflected power at the sidebands, on the other hand, is the same as if the sample were biased far off resonance. Finally, there are no other sideband components.

A step by step procedure for alignment of the dual modulation system is given in Appendix IV-C. Once aligned it is possible to turn up the microwave power level to

measure the spin wave instability threshold. A suppression curve is presented in Figure 4.6 . The data is plotted in decibels for experimental convenience. Data and theory are in reasonable agreement; the data falls slightly below the drawn curve as can be expected at the modulating frequency. Here again, a complete description would require finite time averaging as in Section III. 2 - C.

APPENDIX IV - A

THE TM_{120}^0 CAVITY

The same physical structure as used in the parallel pumping experiment has been employed for transverse excitation of the uniform precession. All dimensions are as shown in Figure 3.9. The only major modification is removal of the mode suppressor. Other changes are in the coupling. The iris has been increased in size and the waveguide has been attached to the cavity rotated 90° from the orientation in the parallel pump experiment.

The field pattern of the TM_{120}^0 mode in a circular cylindrical cavity is described below and shown schematically in Figure 4.7.

$$\underline{h}_r = + 2 h_0 \cos \varphi \frac{J_1(t_{12} \frac{r}{a})}{(t_{12} \frac{r}{a})} \quad (4.30)$$

$$\underline{h}_\varphi = - 2 h_0 \sin \varphi J_1' (t_{12} \frac{r}{a})$$

$$\underline{e}_z = -j \sqrt{\frac{\mu}{\epsilon}} 2 h_0 \sin \varphi J_1 (t_{12} \frac{r}{a})$$

$$\underline{h}_z = \underline{e}_r = \underline{e}_\varphi = 0$$

where $h_0 =$ r.f. magnetic field amplitude at the geometric center

$t_{12} =$ second zero of $J_1(t) = 7.016$

$a =$ radius of cavity

$J_1(t) =$ First order Bessel function

This particular mode consists of a degenerate pair of modes 90° apart in space phase, each of which can be excited independently by irises in the side wall of the cavity. Because the electric field has no transverse components there is no coupling to the coil and only negligible coupling to its support structure. The frequency and Q are perturbed

less ($\Delta f = 70_{\text{mc}}$) than in the TE_{021}^0 mode. With the coil mounted in place the cavity characteristics are as given below.

$$f_0 = 8382. \text{ mc.}$$

$$Q_0 = 4050.$$

$$\beta_0 = 0.939$$

$$Q_{10} = 2085.$$

$$h_0^2 / P_{\text{ic}} = 0.532 \text{ oe.}^2 / \text{ watt}$$

where P_{ic} = incident power

The sample is located at the geometric center of the cavity where the r.f. magnetic field is uniform and linearly polarized.

APPENDIX IV - B

THE MODULATION CIRCUIT

Details of the coil and modulation circuit are the same as in Appendix III - B except as noted below. The complete modulation circuit is shown in Figure 4.8.

In the present experiment the initial frequency and phase are derived from a bridge oscillator. The signal is attenuated and fed to a P I N modulator in the microwave circuit. The same signal is amplified in a modified amateur radio transmitter and fed to the coil. Phase shift is provided by the output tuning capacitor of the transmitter.

APPENDIX IV - C
ALIGNMENT PROCEDURE

The steps for alignment of the dual modulation scheme and observation of the increased instability threshold are enumerated below.

- Step 1: With the sample biased far off resonance, adjust the microwave frequency to the resonant frequency of the cavity.
- Step 2: Align the transverse modulator by adjusting the variable short to eliminate completely the fundamental component (at ω_z) of oscillation in the power observed on a square law detector. One should observe a d.c. level plus a second harmonic in ω_z .
- Step 3: On a spectrum analyzer, measure the sideband power reflected from the cavity.
- Step 4: Bias the sample so that its resonant frequency coincides with that of the cavity.
- Step 5: Measure the reflected power at the center frequency.
- Step 6: Apply the longitudinal modulating field. Adjust the amplitude and phase so that (a) power reflected at the sidebands, $\omega_0 \pm \omega_z$, is the same as in Step 3, (b) power reflected at the center frequency is the same as in Step 5, and (c) no other sidebands are observed.
- Step 7: Increase the incident power until instability is observed using d.c. detection.
- Step 8: Measure the incident power, P_{ic} , and the amplitude, h_z , and frequency, ω_z , of the longitudinal modulating field.

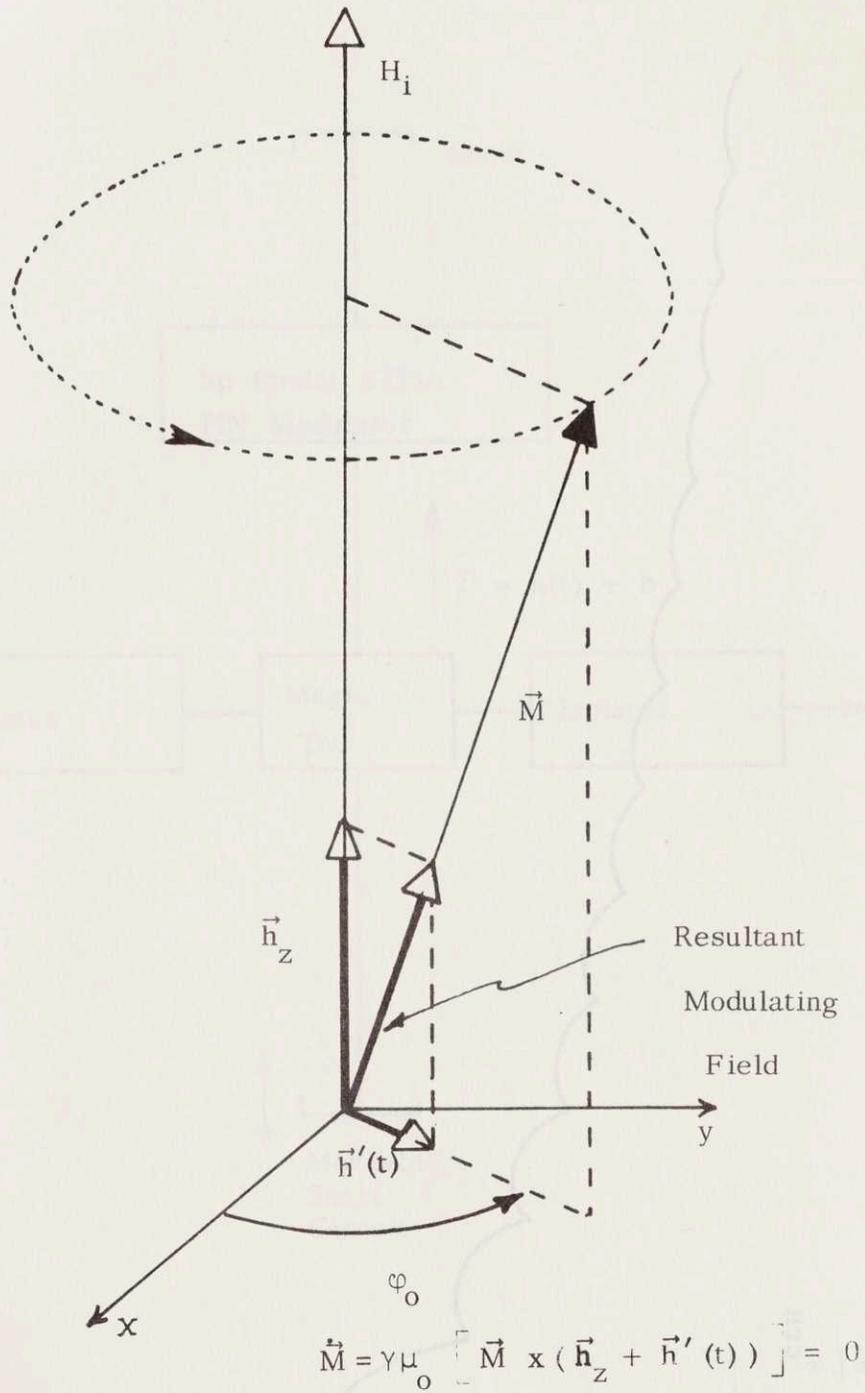


FIGURE 4.1 Dual Modulation

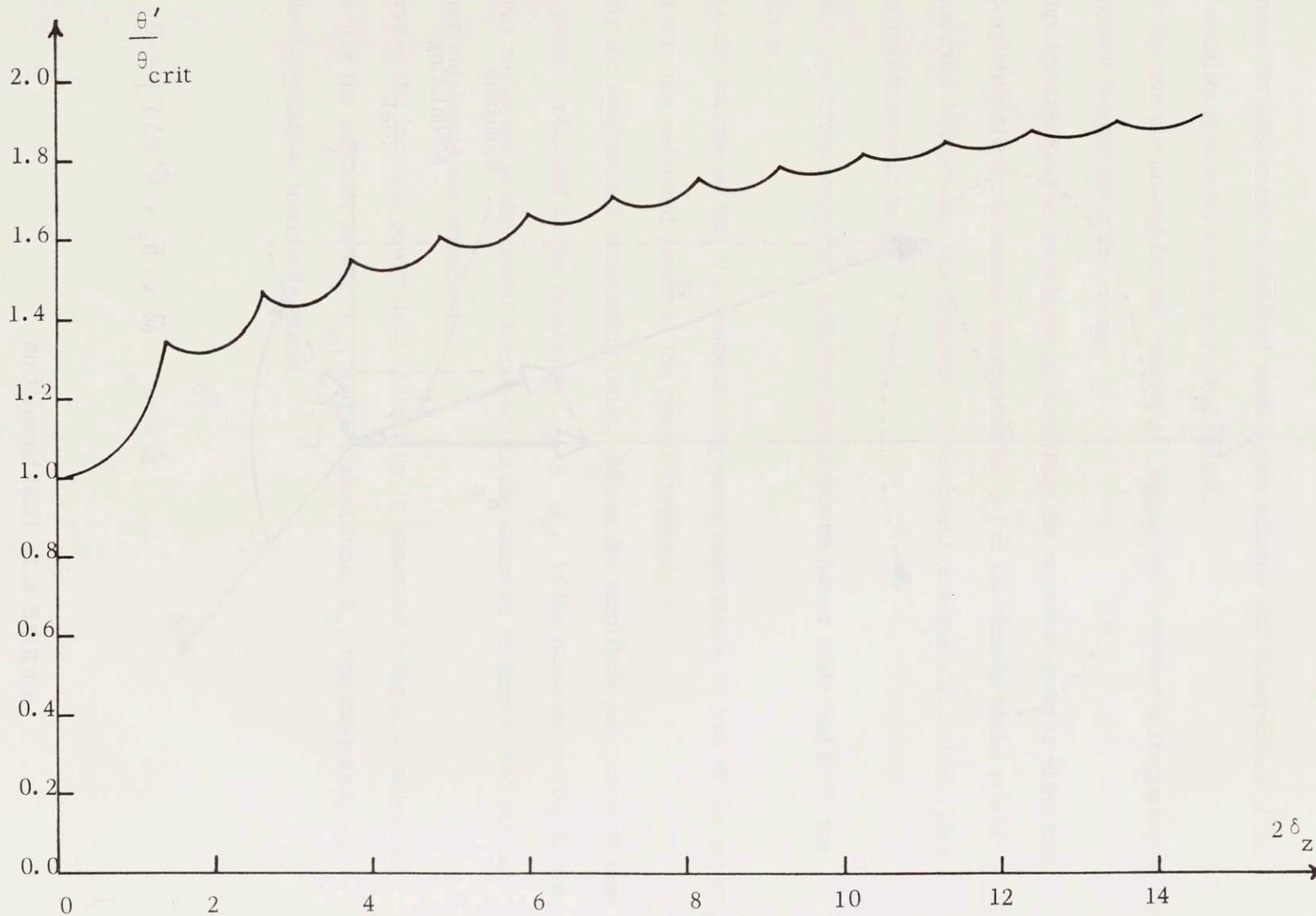


FIGURE 4.2 Suppression
of the Second Order Instability Threshold

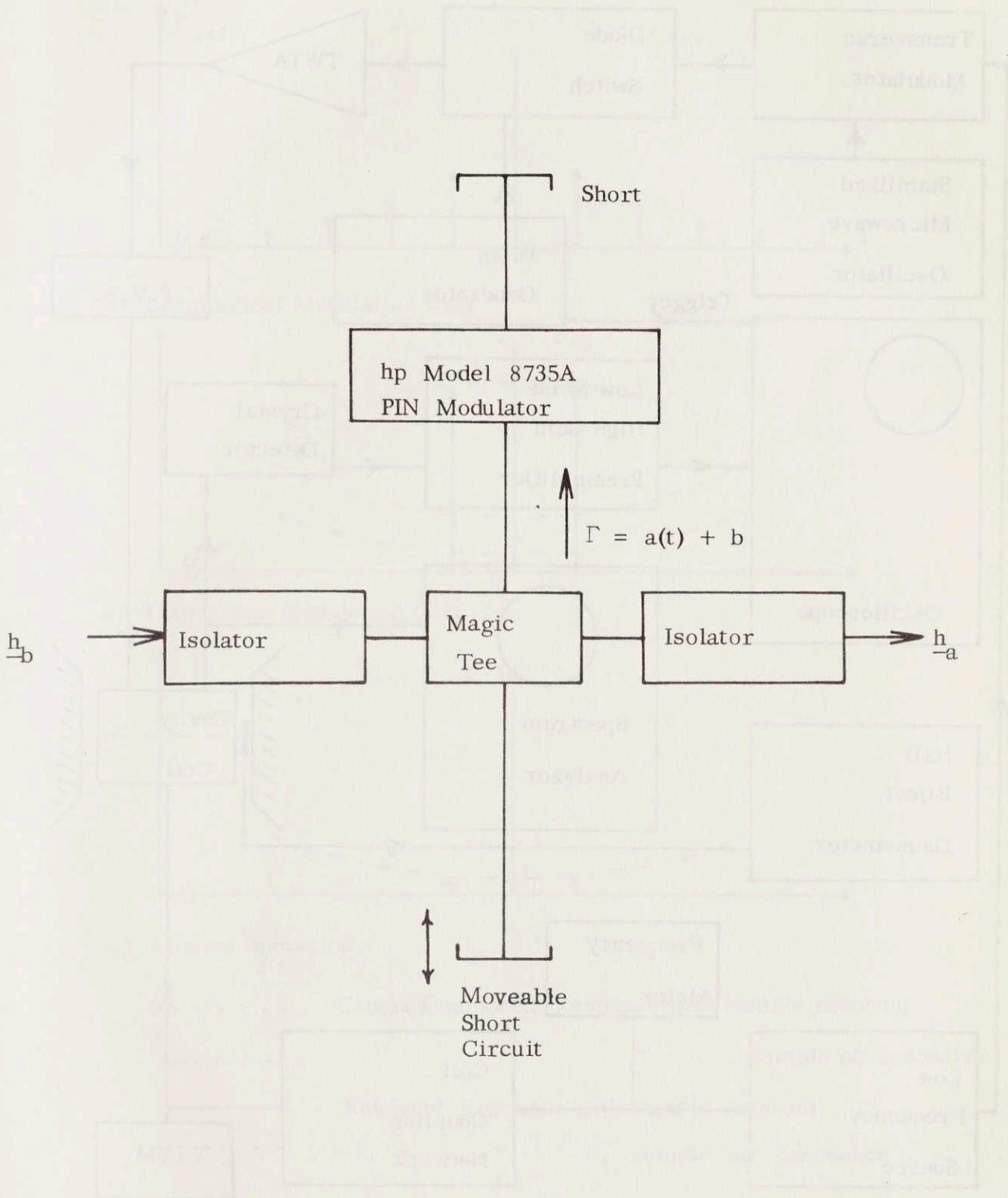


FIGURE 4.3 Transverse Modulator

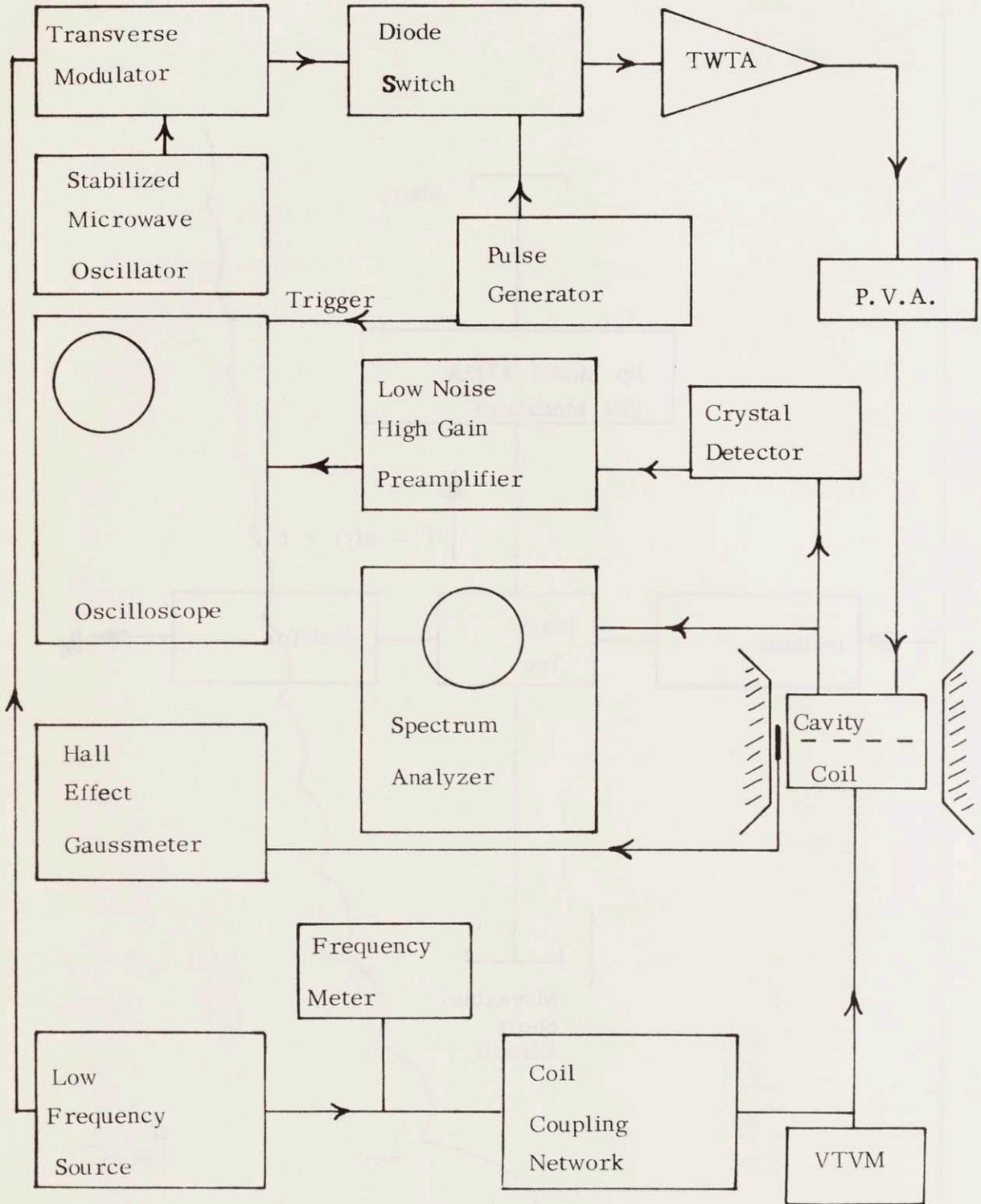
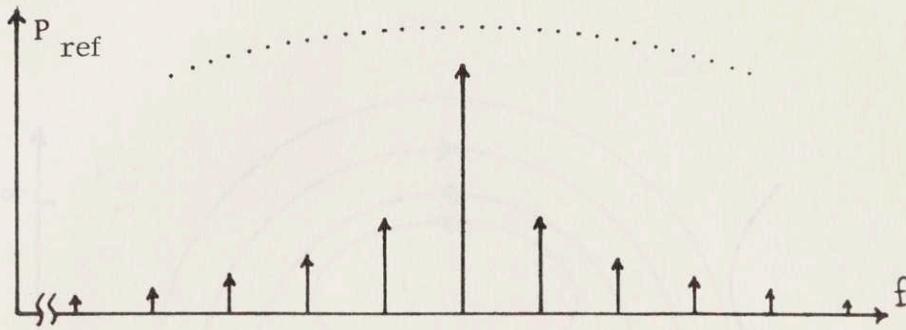
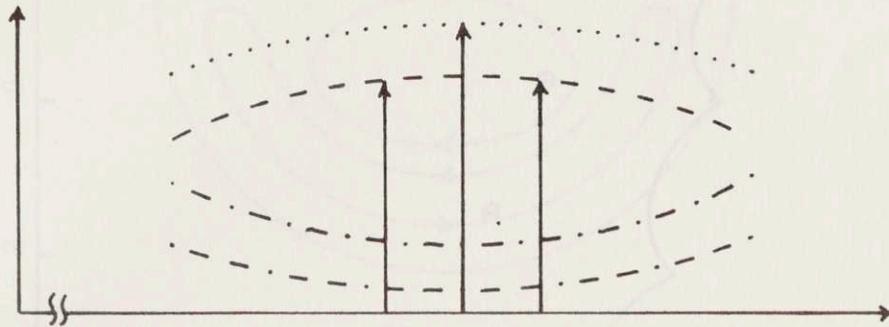


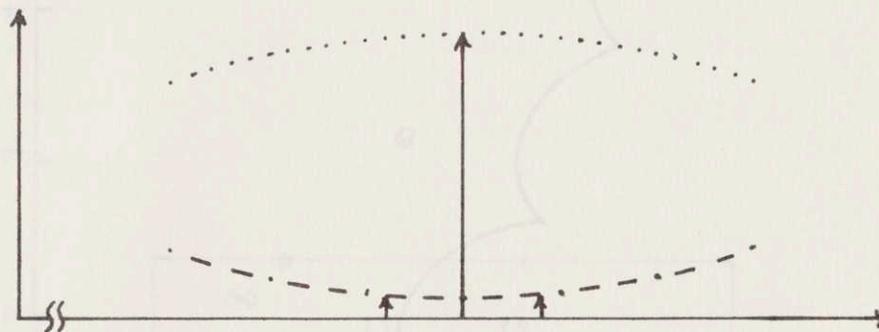
FIGURE 4.4 Block Diagram for Dual Modulation Experiment



a) Longitudinal Modulation Only



b) Transverse Modulation Only



c) Aligned Operation

- Center Component Response with sample resonant
- " " " , sample off resonance
- Sideband Response with sample resonant
- " " " , sample off resonance

FIGURE 4.5 Spectrum of Power Reflected from Cavity

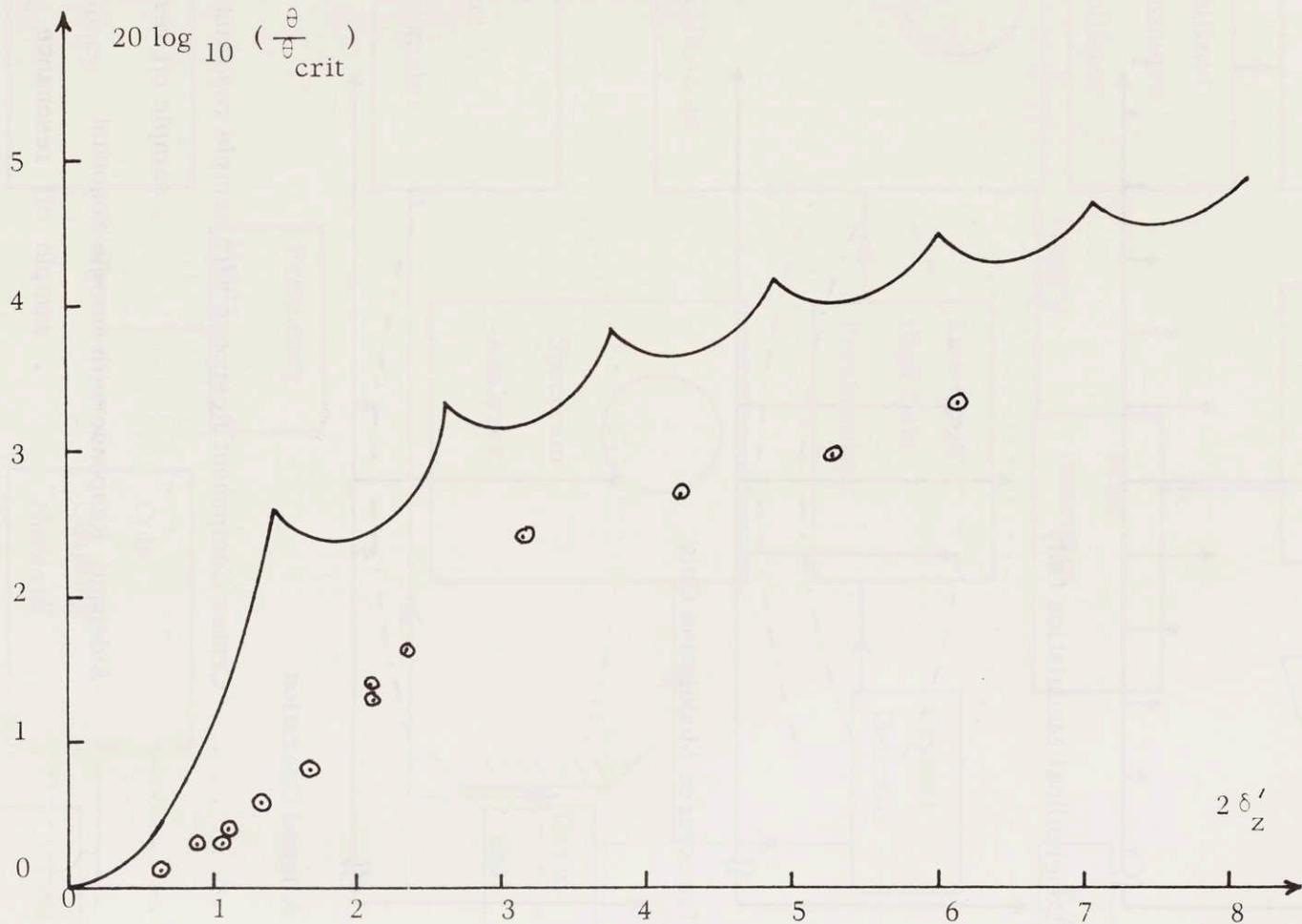
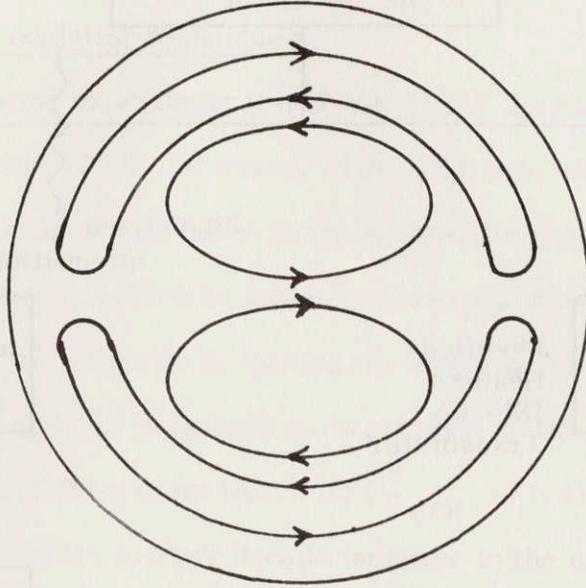
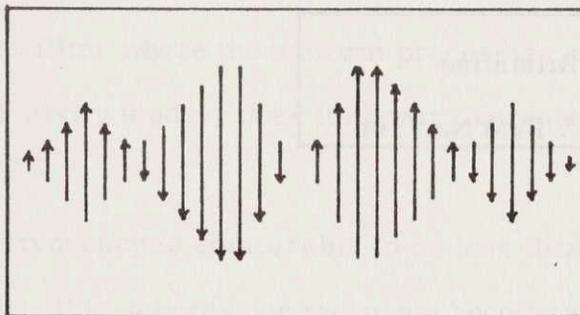


FIGURE 4.6

DB. Increase in Threshold Power



a) End View - Lines of \vec{h} - field



b) Cross section View - Lines of \vec{e} - field

FIGURE 4.7 The electromagnetic fields of a TM_{120}^0 Cavity

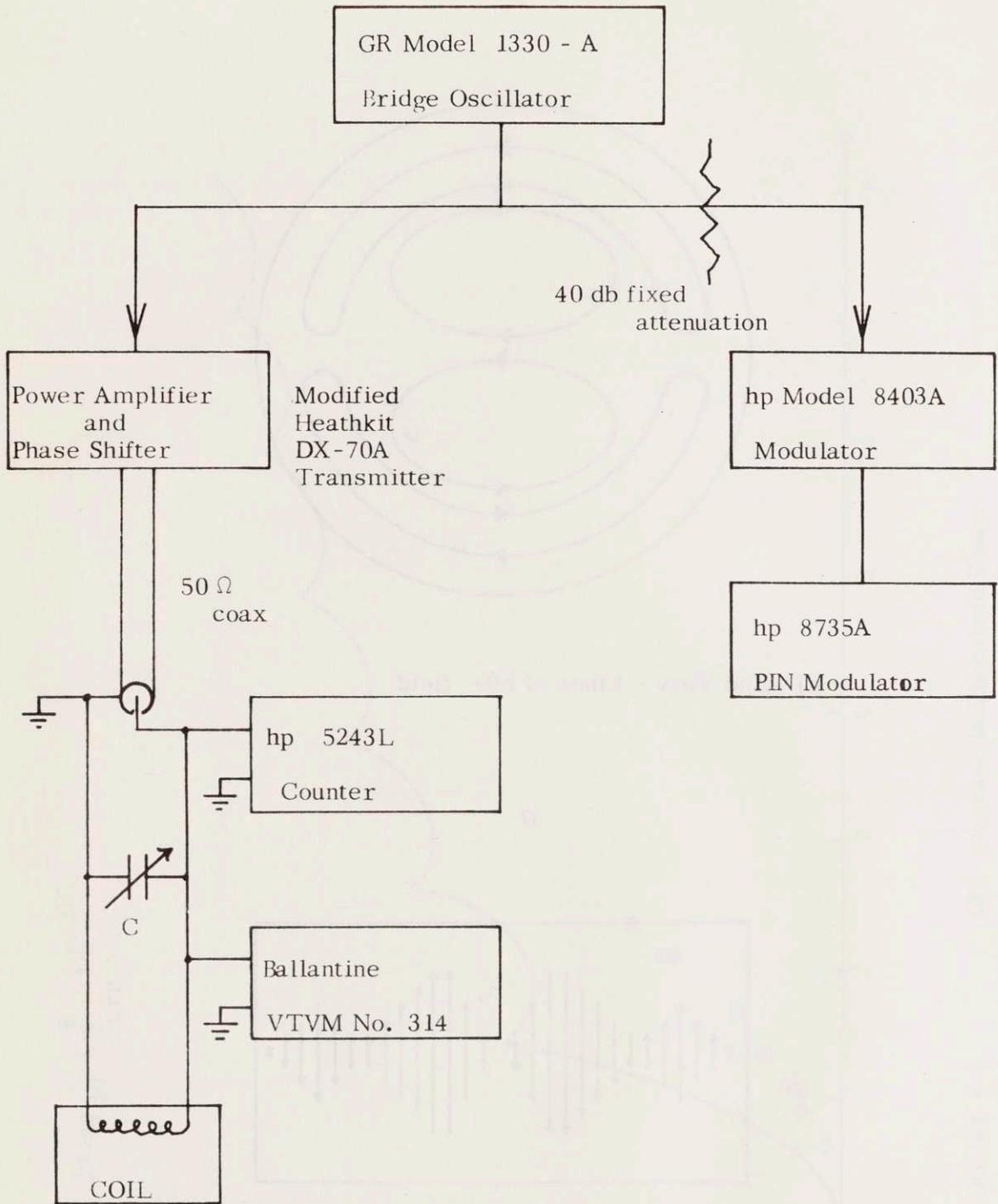


FIGURE 4.8 Dual Modulation Circuit

CHAPTER V

REVIEW AND APPLICATIONS

V.1 Evaluation of modulation techniques

In the parallel pump experiment it has been found possible to raise the threshold for instability by more than 10 db. However, above this level the theory predicts an increase of only 7 db for every decade increase in the modulation parameter, δ_z (see equation 3.15). Thus, this method of suppression becomes increasingly inefficient as the level is raised. Field modulation is less effective in opening the uniform precession (by a factor of 2 when measured in db.) because the threshold is determined by the square of θ . The cone angle has been increased by a little more than 3 db ($\frac{\theta}{\theta_{crit}} = 1.4$). An additional increase can be expected of no more than 3.5 per decade increase in the modulation parameter, δ'_z (equation 4.12).

Use of the field modulation scheme with the uniform precession always involves at least one pair of sidebands. Without the transverse modulation the uniform precession reflects appreciable power back into external circuitry at a large number of sidebands. When the main resonance is properly stabilized there are still, necessarily, sideband components on the incident, and hence as well on the reflected, signals. Only if used in some form of bandpass filter where the uniform precession couples a pair of otherwise uncoupled, degenerate cavity modes, does it appear that an unmodulated output can be transmitted.

If the modulation frequency is comparable to or less than the relaxation frequency, ω_{lk} , of the spin waves, this suppression technique becomes less effective in any configuration. For small δ_z where one excites a center frequency band of spin waves, the quantity $J_0(2\delta_z)$ in the threshold equation [equation (3.14)] must be replaced by the expression in equation (3.24) to account for overlap of the sidebands. This produces

a situation where one must balance various practical considerations. The modulating frequency must be chosen so as to minimize the power delivered to the modulation circuit.

V-2 Applications of modulation suppression

A simple and straightforward application of field modulation can be made in a parallel pump limiter. Spin wave instabilities have been used to limit the power transmitted through a cavity²². Because field modulation introduces no sidebands on the parallel pump driving field, it appears feasible to apply this method in order to achieve electronically variable power limiting. From Figure 3.7 it is apparent that a 10 db variation in transmitted power is possible.

It is expected that extension of the dual modulation scheme to the case where the main resonance has an elliptical precession path will lead to improved harmonic generation. By this method it is possible to drive a resonance of increased amplitude without the generation of sidebands on the precessing magnetization vector. Thus, the harmonic output would be unmodulated.

In any of the parametric amplifiers of Figure 1.2, it must be recognized that there are two transverse modes, both of which would have to be stabilized to prevent sidebands. Dual modulation must then be applied to both of these modes or some other arrangement must be conceived in which the sidebands are self-cancelling. Application of field modulation to just the pump in any of the configurations of Figure 1.2 is insufficient because all transverse modes are affected by a longitudinal field. The idler mode of any of these amplifiers is never coupled to external circuitry and so application of dual modulation to it is impracticable. Furthermore, modulation of the signal mode can only increase the amplifier noise figure. Application of the method of field modulation does not appear to lend itself to application in parametric amplifiers, even for diagnostic purposes.

V.3 Operation below the spin wave manifold

For large amplitude resonance a more interesting possibility appears to be a combination of the thin disc and magnetodynamic coupling experiments described in Section I.3. In practice it is difficult to grow, cut, grind, and polish a single crystal ferromagnetic disc so as to have an aspect ratio, m (diameter/thickness) greater than about twenty. For²² a 3 mil thick by 50 mil diameter disc, $m = 16.7$ and $N_t = 0.044$. Calculation for a disc this size of pure single crystal YIG ($\omega_M = 5$ Gc.) indicates that the uniform precession lies 220 megacycles ($= N_t \omega_M$) above the bottom edge of the spin wave manifold. Now if the uniform precession is driven below resonance at the bottom edge, it follows from equation 2.62 that the cone angle, θ , is less than that at resonance, θ_{res} , by the factor $\left(\frac{\omega_0 - \omega}{\omega_{L0}} \right)$ for the same driving field. For a sample with $2 \Delta H_0 = 0.3$ oe, this factor is 523. thus it would be difficult even to determine if spin wave instabilities are forbidden below this point.

It appears, from a preliminary investigation, that one can selectively couple to and lower the resonant frequency of a single magnetic mode by means of magnetodynamic coupling. An experiment has been carried out in which a 20 mil YIG sphere was excited by the TE_{011}^0 mode of a closed cylindrical rutile resonator. When the d.c. bias field was adjusted so that the sample resonant frequency when uncoupled was equal to the cavity resonant frequency, one resonance was observed shifted down by 375 mc. Theory³⁹ for this shift indicates that it is proportional to the square root of the volume for any low loss ferrite ellipsoid in a uniform field. Extrapolation for the above mentioned disc implies a possible frequency shift of 445. mc, sufficient to drop the uniform precession well below the spin wave manifold. It should, therefore, be possible to investigate spin wave instabilities around the band edge. Analysis is still necessary to determine the cone angle possible for a given driving field as a function of d.c. bias in the coupled system.



77 Massachusetts Avenue
Cambridge, MA 02139
<http://libraries.mit.edu/ask>

DISCLAIMER NOTICE

Due to the condition of the original material, there are unavoidable flaws in this reproduction. We have made every effort possible to provide you with the best copy available.

Thank you.

The following pages were not included in the original document submitted to the MIT Libraries.

This is the most complete copy available.

p. 102

BIBLIOGRAPHY

1. H. Suhl, "The Theory of Ferromagnetic Resonance at High Signal Powers", *J. Phys. Chem. Solids*, 1, pp. 209-227, (1956).
2. E. Schlömann, "Ferromagnetic Resonance at High Power Levels", Raytheon Technical Report, R-48, (1959).
3. F. R. Morgenthaler, "On the General Theory of Microwave Interactions with Ellipsoidal Ferrimagnetic Insulators", M. I. T. Ph.D. Thesis, (May, 1960).
4. M. Sparks, "Ferromagnetic Relaxation Theory", McGraw-Hill Book Company, (1964).
5. R. M. White, "A Theoretical Investigation of the High Power Behavior of Magnetic Insulators", Stanford Ph.D. Thesis, (March, 1964).
6. McLachlan, "Ordinary Non-Linear Differential Equations", Oxford, Clarendon Press, pp. 87-89, (1956), Second Edition.
7. F. R. Morgenthaler, "A Note on Second Order Spinwave Instabilities in Ferrimagnetic Spheroids", Tech. Memo, CRRD-55, AFCRL, Bedford, Mass., (July, 1962).
8. F. R. Morgenthaler, "An Analog Computer Study of Unstable Spin Waves", *J. Appl. Phys.*, 35, pp. 900-901, (1964).
9. F. R. Morgenthaler, "Parallel-Pumped Magnon Instabilities in a Two-Sublattice Ferrimagnetic Crystal", *J. Appl. Phys.*, 36, No. 10, pp. 3102-3111, (October, 1966).
10. R. T. Denton, "Theoretical and Experimental Characteristics of a Ferromagnetic Amplifier Using Longitudinal Pumping", *J. Appl. Phys.*, 32, No. 3, pp. 300S-307S, (March, 1961).
11. R. L. Comstock and E. Hansen, "Analysis of the Nondegenerate Parallel Pumping of Magnetoelastic Waves in Ferromagnets", *J. Appl. Phys.*, 36, No. 5, pp. 1567-1569, (May, 1965).
12. C. P. Hartwig, J. J. Green, R. I. Joseph and E. Schlömann, "Subthreshold Steady-State Absorption under Parallel Pumping", *J. Appl. Phys.*, 36, No. 3, part 2, pp. 1265-1266, (March, 1965).
13. H. Suhl, "Restoration of Stability in Ferromagnetic Resonance", *Phys. Rev. Letters*, 6, pp. 174-176, (1961).
14. T. S. Hartwick, E. R. Peressini and M. T. Weiss, "Suppression of Subsidiary Absorption in Ferrites by Modulation Techniques", *Phys. Rev. Letters*, 6, pp. 176-177, (1961).
15. J. F. Ollom and H. L. Goldstein, "Effect of Frequency Modulation on Subsidiary Resonance in Ferrites", *J. Appl. Phys.*, 32, No. 10, p. 2059, (October, 1961).

16. F. R. Morgenthaler, F. A. Olson and G. E. Bennett, "Suppression of Spin Wave Instabilities Associated With Ferromagnetic Resonance", *J. of Phys. Soc. of Japan*, 17, Supp. B-I, (1962).
17. J. F. Ollom and H. L. Goldstein, "Relation of Spin Wave Linewidth to Optimum Modulating Frequency Required for Suppression of Subsidiary Resonance in Ferrites", *A. P. Letters*, 2, No. 9, (May 1, 1963).
18. W. E. Courtney and P. J. B. Clarricoats, "Experimental Studies of Spin Waves Excited by Parallel Pumping", *J. Electron. and Contr.*, 16, No. 1, pp. 1-20, (January, 1964).
19. Harvard Univ., Computation Laboratory Annals, Vols. 3-14, Tables of the Bessel functions of the first kind of orders zero to one hundred thirty-five, (1947).
20. G. Feher, "Sensitivity Considerations in Microwave Paramagnetic Resonance Absorption Techniques", *Bell System Technical Journal*, 36, No. 2, pp. 449-484, (March, 1957).
21. L. C. Bahiana and L. D. Smullin, "Coupling of Modes in Uniform, Composite Waveguides", *I. R. E. Trans.*, MTT-8, pp. 454-458, (1960).
22. B. Lax and K. J. Button, "Microwave Ferrites and Ferrimagnetics", McGraw-Hill Book Company, Chapt. 4, (1962).
23. M. Weger, "Passage Effects in Paramagnetic Resonance Experiments", *Bell System Technical Journal*, 39, pp. 1013-1112, (1960).
24. P. W. Anderson, "The Reaction Field and Its Use in Some Solid-State Amplifiers", *J. Appl. Phys.*, 28, pp. 1049-1053, (September, 1957).
25. J. J. Green, "Microwave Resonance in Ferromagnetic Systems at High-Signal Levels", Gordon McKay Laboratory Scientific Report No. 2 (Series 2), Harvard University, December 1, 1959.
26. P. E. Seiden, "Ferrimagnetic Resonance in Polycrystalline YIG", Microwave Laboratory Report No. 657, Stanford University, October, 1959.
27. E. Schlomann, J. J. Green, U. Milano, "Recent Developments in Ferromagnetic Resonance at High Power Levels", *JAP supp.*, 31, No. 5, pp. 386-395, May, 1960.
28. H. Suhl, "Theory of the Ferromagnetic Microwave Amplifier", *JAP*, 28, November, 1957, pp. 1225-1236.
29. A. D. Berk, L. Kleinman, C. E. Nelson, "Modified Semistatic Ferrite Amplifier 11, IRE Wescon Convention Record 2, Part III, p. 9, (1958).
30. R. W. Damon, J. R. Eshbach, "Theoretical Limitations to Ferromagnetic Amplifier Performance", *IRE Trans. MTT-8*, No. 1, pp. 4-9 (1960).

31. R. T. Denton, "Longitudinal Pumping on Ferromagnetic Materials with application to a New Type of Microwave Parametric Amplifier," Ph.D. Dissertation, Univ. of Michigan, 1960.
32. E. R. Peressini, T. S. Hartwick, M. T. Weiss, "An Experimental Study of the Parallel Pumped Ferromagnetic Amplifier", HAP, 33, No. 11, pp. 3292-3295, November, 1962.
33. R. W. Roberts, B. A. Auld, R. R. Schell, "Magnetodynamic Mode Ferrite Amplifier", JAP supp., 33, No. 3, pp. 1267-1268, March, 1962.
34. P. H. Cole, "Energy Exchange and Loss Properties of Ferrites for Parametric Amplifiers", Ph. D. Dissertation, U. of Sidney, Australia, 1964.
35. S. G. Liu, "An Investigation of Spin Wave Suppression in Ferrites", Microwave Laboratory Report No. 1092, Stanford University, October, 1963.
36. W. H. Steier, "Magnetodynamic Dipolar Ferrite Modes", Ph. D. Dissertation, University of Illinois, 1960.
37. F. R. Morgenthaler, "On the Possibility of Obtaining Large Amplitude Resonance in Very Thin Ferrimagnetic Disks", JAP supp., 33, No. 3, pp. 1297-1299, March, 1962.
38. R. E. Tokheim, "Saturation Phenomena in Zn_2Y Ferrite at Frequencies below Resonance", Microwave Laboratory Report No. 1290, Stanford University, February, 1965.
39. C. P. Hartwig, "Linear Coupling to Magnetic Modes of Resonance," Microwave and Quantum Magnetics Group Technical Report No. 6, June, 1966.
40. P. H. Cole, private communication

BIOGRAPHICAL NOTE

The author was born in Boston, Massachusetts on July 13, 1939. He received his high school education at the Boston Public Latin School. As an undergraduate at the Massachusetts Institute of Technology, he participated in the cooperative course in electrical engineering and carried out work assignments at Bell Telephone Laboratories, Incorporated, Murray Hill and Whippany, New Jersey.

In June, 1962, the author received the S.B. and the S.M. degrees in electrical engineering. From February, 1962, to June, 1966, he has held the positions of teaching and research assistant in E.E. During the summer of 1964, he joined the Research Division of Raytheon Manufacturing Company as a Research Scientist.

The author has held a Boston Kiwanis Club Scholarship (1957-58), a Freshman Competitive Scholarship (1957-58), an Edwards Scholarship (1957-1961), a Melvin Scholarship (1958-1961), and a National Science Foundation Teaching Fellowship (1964). In 1961, he was made an honorary student member of the American Society for Testing and Materials. He is a member of Hexalpha, Eta Kappa Nu, Tau Beta Pi, Sigma Xi, the I.E.E.E. and the American Physical Society.

Publications are:

"Subthreshold Steady-State Absorption under Parallel Pumping" by C.P. Hartwig, J.J. Green, R.I. Joseph and E. Schlomann, JAP, 36, No. 3 (part 2) March, 1965, pp. 1265-1266.

"Transient Growth of Spin Waves under Parallel Pumping" by R.I. Joseph, C.P. Hartwig, T. Kohane, and E. Schlomann, JAP, 37, No. 3, 1 March, 1966, pp. 1069-1070.